

I. R. Paterson (russell.paterson@deb.uminho.pt)

1. I am unclear how the data in Paterson et al. (2015) supported LULC change in Indonesia as was stated in the manuscript. The authors should clarify.

Line 718 (in the discussion): Paterson et al. (2015) mention that the LST in Malaysia increased over the last four decades of 2.7 – 4.0 degrees C per 100 years. This is an example of LST change in another region close to Indonesia. However, this is not from first hand observation, data or research but results from the Malaysian Meteorological Department. We admit that this reference is misplaced here and removed the reference to Paterson et al. (2015) from the discussion.

2. They could also write LULC in full at first with the abbreviation in brackets afterwards.

We realize that the abbreviation LULC is introduced in line 600 and that it was not defined anywhere else. We added the full words followed by the abbreviation in line 600 as “LST patterns across different land use and land cover (LULC) types.

3. The English could be tightened up in parts of the paper.

a. E.g. they start sentences with "We" on lines 31 and 34. Also, this is not the passive voice. Similarly, "Our" lines 40 and 43.

We have tried to improve the English in the manuscript, removing the repeated words in the same paragraph, such as the “we” or “our” in the indicated lines. We have especially tightened the abstract, but kept it in active voice, as the Biogeosciences’ guidelines do not explicitly mention the preferred style of writing.

b. Line 57: "in the past decades" is imprecise and clumsy.

We changed this to “in the past two and a half decades” to refer to our study period 2000 - 2015

c. Lines 66-69: Three "and"s are used in this sentence. Not the best English.

The biophysical variables (albedo, emissivity and surface roughness) affect gas and energy exchange processes between the land surface and the atmosphere. We did not find any obsolete “and” in this construction.

d. Line 75: Replace "rise" with "increase".

We changed the verb as suggested.

e. Line 94-96: You should not have to explain what the "vice versa" is.

We removed the “vice versa” and connected the remaining sentence to the previous. We wanted to describe both situations of ET increase and ET decrease: what happens when ET increases and when ET decreases. The rephrased sentence is now: “In case ET is decreased, surface temperatures and fluxes of sensible heat (H) increase. On the other hand, when ET increases, increased LE fluxes lower surface temperatures and decrease H fluxes (Mahmood et al., 2014).”

f. Anyway, I will stop there as its too much work to point out other such smallish things. Maybe you consider these unimportant...

We thank Dr. Paterson for his comments and suggestions for improvements. We are happy to incorporate the suggested language corrections. Additionally, we reread the entire manuscript and made further English correction.

II. A. RIVAL (alain.rival@cirad.fr)

1. Given the nature, impact and extend of results presented the paper submitted by Sabajo et al, the present title of article clearly appears as unapropriate. Indeed results do not show any pivotal role for oil palm cultivation which should support the assumption that it is a key driver of phenomena observed. The title should stick only to facts and findings, which tend to evidence a difference between native forest and cultivated land in terms of land surface temperature.

We agree with Dr. Rival that the title is too general. Our study shows results from Jambi province/Indonesia only, thus we now mention this specifically in the title. We however think that the evidence from our study is sufficient to link the observed increase of land surface temperature to the expansion of oil palm and other cash crops as the observed temperature increase at provincial level is in line with the observed temperature differences across land use type and the expansion of oil palm and cash crops over the last two and a half decades in the Jambi province. The area cultivated with oil palm grew faster than the area cultivated with rubber plantations between 1990 and 2011 (Clough et al. 2016). The title of our article is now: "Expansion of oil palm and other cash crops cause an increase of the surface temperature of the Jambi province in Indonesia"

III. Anonymous Referee #1

General: The authors investigate the effect of land cover change (from forests to 'other' and mostly oil palm plantations) on regional land surface temperatures. They use remote sensing to determine LST (and albedo, NDVI, and ET). They conclude that conversion from forests had led to a ~ 1 degree C temperature (positive) change after accounting for albedo. They also conclude that this is a positive feedback to climate warming.

1. I only suggest some minor edits and (if the authors can) and expansion of the discussion of what these LST changes might translate to in the atmosphere?

The reviewer brings up an important issue of land surface – atmosphere feedback. A recent study by Tölle et al. (2016)[#] showed for SE Asia as a whole that land use change at large scale impacts the boundary layer structure, cloud-cover regime and other aspects of local and regional weather and climate. Particularly, land clearings can amplify the response to climatic extreme events such as El Nino Southern Oscillation. Analyzing this kind of effects require however a regional climate model, which is beyond the scope of our study. We now discuss this aspect in the manuscript and added the following sentence:

Line 773: "A recent study by Tölle et al. (2017) showed for SE Asia that land use change at large scale may increase not only surface temperature but also impact other aspects of local and regional weather and climate occurring also in regimes remote from the original landscape disturbance. Land clearings can amplify the response to climatic extreme events such as El Nino Southern Oscillation."

[#]Tölle, M. H., Engler, S., and Panitz, H. 2017: Impact of Abrupt Land Cover Changes by Tropical Deforestation on Southeast Asian Climate and Agriculture. *Journal of Climate*, **30(7)**, 2587 – 2600, doi: 10.1175/JCLI-D-16-0131.1.

2. How much larger of a region will they affect? How would you determine this?

This study focuses on local and effects at the provincial level. Estimating or predicting the effects at a larger regional scale also requires a regional climate model as used in the study of

Tölle et al. (2017). Tölle et al. (2017) show that the effects of land use changes occur in remote regions other than where the land use changes occur. These effects are caused by the impacts the land cover change has on El Niño/La Niña episodes thereby enhancing wetter conditions in other regions, whereas in other regions wetter conditions decrease.

Introduction: nicely written and I appreciate the well thought out definitions.

3. Line 96: missing an “as” after “such”.

We added the missing word as suggested.

4. Methods: Could you describe the study sites in a little more detail (rather than the reference Drescher).

We added the following information:

*L. 186: “Previously logged rainforests in the Jambi province have been converted into intensively managed agro-industrial production zones as well as into smallholder farms to grow cash crop trees of rubber (*Hevea brasiliensis*) and oil palm (*Elaeis guineensis*) or fast-growing tree species such as *Acacia mangium* for pulp production (Drescher et al., 2016). The area cultivated with oil palm grew faster than the area cultivated with rubber plantations between 1990 and 2011 (Clough et al. 2016).”*

5. ET calculations: I’m familiar with the use of satellite data for all of the variables except for ET. Did you compare ET with the tower sites? How well does it work?

I see that you added this to the supplement, but it would be nice to have a validation of this method explained in the main text.

We have ET and LE estimates from eddy covariance measurements for two oil palm plantations in Jambi Province (young and mature oil palm plantation). Our SEBAL based LE estimates are within the variability range of LE measured from eddy covariance under similar meteorological conditions.

We added the following text: “The SEBAL based LE estimates are within the variability range of LE measurements using the eddy covariance technique under similar meteorological conditions (see SI).”

6. Results: Line 405-406: Hot = red? And cool = Blue colors. Can you please specify this?

In our description of the figure we added the matching colors as suggested. Line 405 – 406: “the hot areas (red) correspond to the known clear-cut areas, urban areas or other sparsely vegetated areas, the cooler areas (blue) correspond to vegetated areas such as forest, plantation forests and mature oil palm plantations.”

7. Discussion: Line 668: When I look at the figures, there also seems to be a high correlation between NDVI and ET (simply because the response pattern, the pattern of the changes, look very similar). Can you explain this? Is it because of the ET calculation?

Yes, ET and NDVI are highly correlated on one hand because the NDVI is used in the calculation of ET. On the other hand, another input for ET is LST, which is calculated from the raw thermal band (L6). L6 and NDVI are also highly correlated ($r = -0.87$) (see table 2, Line 494 – 502) even though NDVI and L6 are derived/measured from independent satellite bands. Thus, it come as no surprise that there is a correlation between NDVI and ET.

8. Line 763: “concurrent to” should be “concurrent with”

We changed the sentence with the correct prepositions as suggested.

9. Line 768: “governmental” should be “government”

We changed this and used the correct word.

Final remarks: This is a well-written, well-organized manuscript. I support publication in Biogeosciences.

We thank the anonymous referee for reviewing the manuscript and for the suggestions to improve the manuscript.

IV. Anonymous Referee #2

General comments: Sabajo et al. evaluates the impact of land use changes on land surface temperatures in Indonesia over the MODIS timespan (1999-2015). The study is well written and provides a good, long-term observational analysis clearly showing the impact of regional deforestation on increasing land surface temperature across an entire region.

We thank the anonymous referee for reviewing the manuscript and for the suggestions to improve the manuscript.

1. The only general comment I have is that it would be good to include a **seasonality analysis** showing how deforestation has changed land surface temperature in both wet and dry season. I know that satellite remote sensing is more challenging during the wet season, but I think evaluating the impact of land changes with seasonality would be useful. This could also highlight likely reductions in ET with land change (and shallower rooting zones) during the dry season. The dry season is also when heat impacts (including wildfires) could be more significant.

We agree that a seasonality analysis might show differences between the wet and dry season. We now made a seasonality analysis. Overall, the relationships in the dry season are stronger than for the wet season as we have much more usable data during the dry season. We found significant differences between LST of the dry and wet season. At 10:30 am the LST increased 0.09 ± 0.02 °C per year during the dry season, while the increase during the wet season was lower (0.06 ± 0.02 °C per year) (Fig. S10.1). Around 1:30 pm the LST increased 0.08 ± 0.03 °C per year, against 0.03 ± 0.02 °C increase per year during the wet season. At 10:30 pm the LST increased 0.03 ± 0.01 °C per year in the dry season, compared to a LST increase of 0.02 ± 0.01 °C in the wet season. At 1:30 am, the LST increased 0.05 ± 0.02 °C in the dry season, while the LST during the wet season increased 0.05 ± 0.03 °C. The increase of the LST at 1:30 pm, 10:30 pm and 1:30 am in the wet season was not significant ($p = 0.12$, $p = 0.06$ and $p = 0.11$, respectively). The significant increase of the LST during the dry season at all 4 times of observations suggests that the warming is more pronounced during the dry season compared to the wet season, which is reasonable as we have more incoming radiation during the dry season. Nevertheless, we prefer to pool the data from the dry and the wet season in order to get more statistically robust relationships.

In our analysis of the MODIS LST data we have not come across anomalous LST that could be attributed to forest fires. This is caused by the mask we applied in selecting the best quality pixels which mostly also removed pixels covered by smoke. A seasonality analysis is not possible with Landsat data because there is not enough data.

We added the following sentence to the manuscript (line 755):

“We like to point out that our MODIS analysis has a larger proportion of data from the dry season compared from the wet season, as there were more cloud free conditions during the dry season. Thus, our reported warming effect reflects cloud free conditions. During cloudy conditions, particularly in the wet season, the warming effect is expected to be lower.”

We also added the seasonal analysis to the supplementary information (S10).

We thank the anonymous referee for reviewing the manuscript and for the suggestions to improve the manuscript.

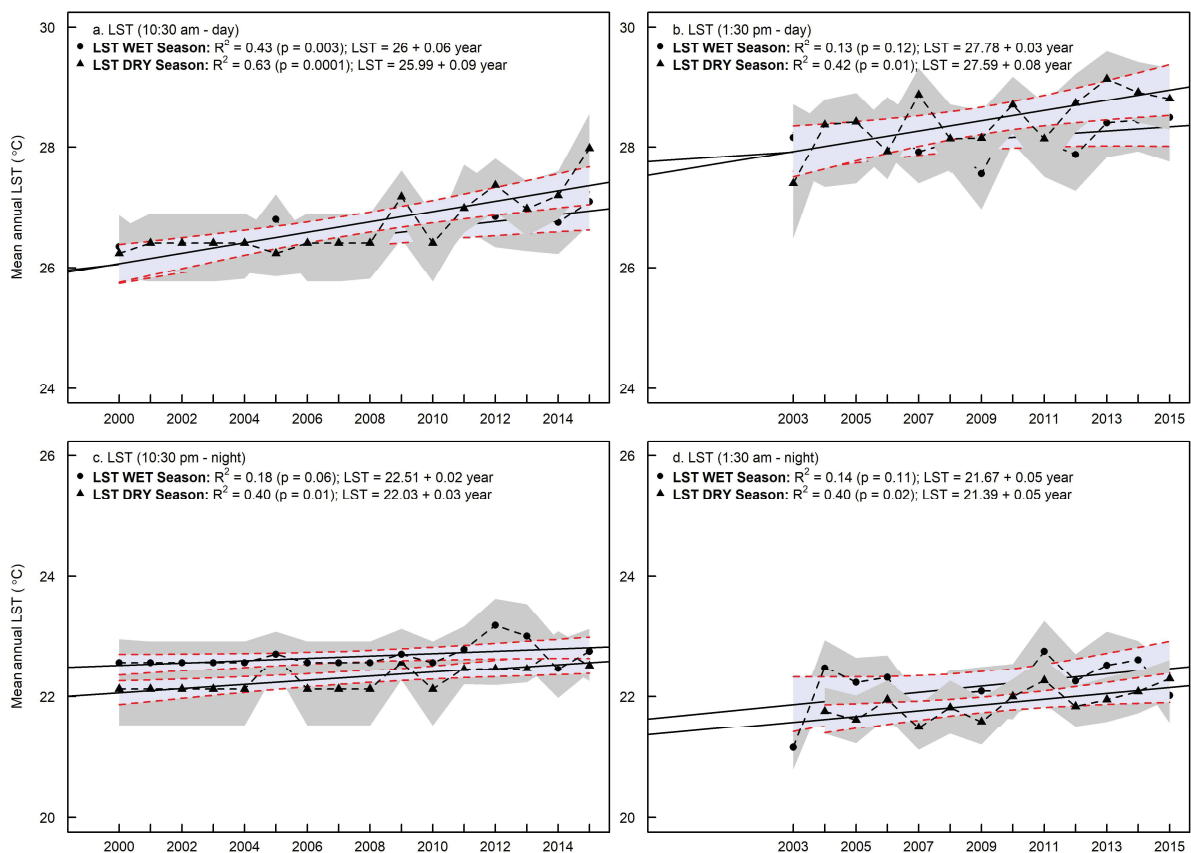
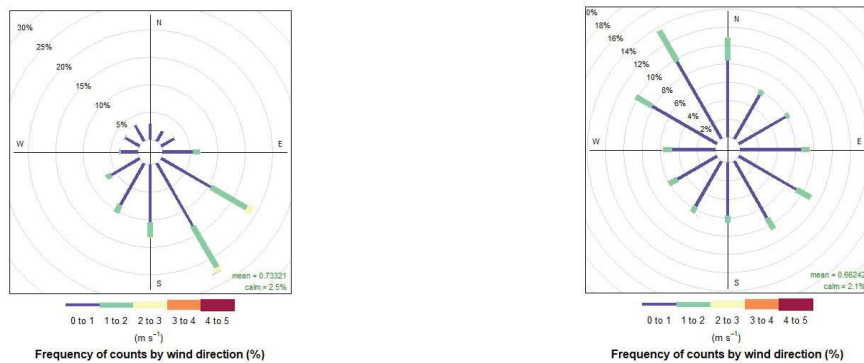


Fig. S10.1 (from manuscript, extended): Wet and dry season are separated.

Wet season: All months except June – September/October; Dry season: June – September/October (Meijide et al., 2017 & Drescher et al., 2016).

This figure has been added to the Supplementary Information (S10)

2. Specific comments: For Figure 1 (and text in the manuscript related to Figure 1), it might be good to describe the general atmospheric circulation for wet and dry seasons (are winds from the east or from the west). This would help the reader evaluate whether there are substantial land use changes upwind of the forest plots that are used as the baseline “control” to evaluate land surface temperature changes to due land use changes and not overall global climate change. *We include a wind rose from one of our reference meteorological stations in the area, (see Drescher et al., 2016), for data collected between October 2013 to May 2016. Based on the climate diagram for the region (obtained from data from 1991-2011) we considered as the dry season the months of June-September and the rest was considered as wet season. See the wind roses for the dry (left) and wet (right) seasons below:*



During the dry season counts by winds were predominantly from the SE, whereas during the wet season winds were predominantly from the NW. The SE vs. NW shift in wind directions is in line with the regional monsoonal circulation. The landscape in the lowland of Jambi province is, however, very patchy with small-scale mosaics of different land uses. While we cannot fully rule out that advection from upwind land use changes may play a role, but it seems unlikely to have a systematic bias given the typical patchiness of the landscape. Also warm air advection would mean that the “climate change” warming of the forested “control” site is overestimated, thus making the land-use change effect even larger.

V. List of major changes

1. We have changed the title to: “*Expansion of oil palm and other cash crops cause an increase of the surface temperature of the Jambi province in Indonesia*”. The first title was too general, the results apply to the Jambi province and not to the whole of Indonesia.
2. We removed the reference of Paterson et al. (2015). After re-reading we concluded that this reference was not correctly cited and misplaced.
3. We added a new reference of Tölle et al. (2017). This reference was a new publication that complemented our results with a modelling approach.
4. We added 1 section to the supporting information (S10). S10 contains a seasonality analysis as suggested by anonymous referee #2. We also add a short sentence in the discussion and refer to the S10 for the results of the analysis.
5. Equations 9 – 11 have been renumbered from 10 – 12, due to a mistake in the equation 9 (which was by accident numbered as 1, while in fact that had to be equation 9).

6. We changed figure 5: we only adjusted the legend and paid attention to the rounding of the numbers in the equations.

1 **Expansion of oil palm and other cash crops causes an increase of land surface temperature**
2 **of the Jambi province in Indonesia**

3
4 Clifton R. Sabajo^{1,2†}, Gueric le Maire³, Tania June⁴, Ana Meijide¹, Olivier Roupsard^{3,5},
5 Alexander Knohl^{1,6}

6
7 ¹ University of Goettingen, Bioclimatology, 37077 Göttingen, Germany

8 ² AgroParisTech – Centre de Montpellier, Agropolis International, 648 rue Jean-François
9 Breton, 34093 Montpellier, France

10 ³ CIRAD, UMR Eco&Sols, F-34398 Montpellier, France

11 ⁴ Agrometeorology Laboratory Department of Geophysics and Meteorology,

12 Faculty of Mathematics and Natural Sciences, Bogor Agricultural University (IPB), Indonesia

13 ⁵ CATIE (Centro Agronómico Tropical de Investigación y Enseñanza / Tropical Agriculture
14 Centre for Research and Higher Education), 7170 Turrialba, Costa Rica

15 ⁶ University of Goettingen, Centre of Biodiversity and Sustainable Land Use (CBL), 37073
16 Goettingen, Germany

17
18 † Correspondence: Clifton R. Sabajo, University of Goettingen, Bioclimatology, Büsgenweg 2,
19 37077 Göttingen, Germany. E-mail: csabajo@uni-goettingen.de

20 Telephone: +49 (0) 551 39 12114

21
22
23 **Abstract**

24
25 Indonesia is currently one of the regions with the highest transformation rate of the land surface
26 worldwide due to the expansion of oil palm plantations and other cash crops replacing forests
27 on large scales. Land cover changes, which modify land surface properties, have a direct effect

28 on the land surface temperature (LST), a key driver for many ecological functions. Despite the
29 large historic land transformation in Indonesia toward oil palm and other cash crops and
30 governmental plans for future expansion, this is the first study so far to quantify the impact of
31 land transformation in Indonesia on LST. We analyse LST from the thermal band of a Landsat
32 image and produce a ~~high-resolution~~high-resolution surface temperature map (30m) for the
33 lowlands of the Jambi province ~~in~~ Sumatra (Indonesia), a region ~~of which suffered~~ large land
34 transformation towards oil palm and other cash crops over the past decades. ~~We~~The
35 ~~comparison of~~ LST, albedo, Normalized Differenced Vegetation Index (NDVI), and
36 evapotranspiration (ET) ~~of between~~ seven different land cover types (forest, urban areas, clear
37 cut land, young and mature oil palm plantations, acacia and rubber plantations). ~~and shows~~ that
38 forests have lower surface temperatures than these land cover types, indicating a local warming
39 effect after forest conversion. ~~with~~ LST differences ~~were~~ up to 10.09 ± 2.6 °C (mean \pm SD)
40 between forest and ~~clear-cut~~clear-cut land. The differences in surface temperatures are
41 explained by an evaporative cooling effect, ~~which offset~~offsetting the ~~an~~ albedo warming
42 effect. Our analysis of the LST trend of the past 16 years based on MODIS data, shows that the
43 average daytime surface temperature of the Jambi province increased by 1.05 °C, which
44 followed the trend of observed land cover changes and exceed the effects of climate warming.
45 ~~Our~~This study provides evidence that the expansion of oil palm plantations and other cash
46 crops leads to changes in biophysical variables, warming the land surface and thus enhancing
47 the increase in air temperature due to climate change.

48

49

50 *Keywords:* Land surface temperature, albedo, NDVI, evapotranspiration, biophysical variables,
51 oil palm, remote sensing, Landsat, MODIS, Indonesia, land-use / land cover change

52

53

54 1 Introduction

55

56 Indonesia is one of the regions where the expansion of cash crop monocultures such as acacia
57 (timber plantation), rubber, oil palm plantations and smallholder agriculture has drastically
58 reduced the area of primary forest in the ~~past~~ last two and a half decades (Bridhikitti and
59 Overcamp, 2012; Drescher et al., 2016; Marlier et al., 2015; Miettinen et al., 2012; Verstraeten
60 et al., 2005). This large scale conversion of rainforest for agricultural use has been observed on
61 the island of Sumatra, which has experienced the highest primary rainforest cover loss in all of
62 Indonesia (Drescher et al., 2016; Margono et al., 2012; Miettinen et al., 2011). Forest cover in
63 the Sumatran provinces of Riau, North Sumatra and Jambi, declined from 93 to 38% of
64 provincial area between 1977 and 2009 (Miettinen et al., 2012). These large scale
65 transformations, observed as land cover change, and land-use intensification have led to
66 substantial losses in animal and plant diversity, and ecosystem functions and changed
67 microclimatic conditions (Clough et al., 2016; Dislich et al., 2016; Drescher et al., 2016).
68 Additionally, these changes directly alter vegetation cover and structure as well as land surface
69 properties such as albedo, emissivity, and surface roughness which affect gas and energy
70 exchange processes between the land surface and the atmosphere (Bright et al., 2015).

71

72 Replacing natural vegetation with another land cover modifies the surface albedo, which affects
73 the amount of solar radiation that is absorbed or reflected and consequently alters net radiation
74 and local surface energy balance. A lower or higher albedo results in a smaller or greater
75 reflection of shortwave radiation. As a result, the higher or lower amounts of net radiation
76 absorption may ~~increase~~ rise or ~~lower~~ decrease the surface temperature and change
77 evapotranspiration (Mahmood et al., 2014).

78

79 Changes in land cover also alter surface emissivity, i.e. the ratio of radiation emitted from a
80 surface to the radiation emitted from an ideal black body at the same temperature following the
81 Stefan–Boltzmann law. Emissivity of vegetated surfaces varies with plant species, density,
82 growth stage, water content and surface roughness (Snyder et al., 1998; Weng et al., 2004). A
83 change of emissivity affects the net radiation because it determines the emission of longwave
84 radiation that contributes to radiative cooling (Mahmood et al., 2014).

85

86 Water availability, surface type, soil humidity, local atmospheric and surface conditions affect
87 the energy partitioning into latent (LE), sensible (H) and ground heat (G) fluxes (Mildrexler et
88 al., 2011). Surface roughness affect the transferred sensible and latent heat by regulating vertical
89 mixing of air in the surface layer (van Leeuwen et al., 2011) thereby regulating land surface
90 temperature (LST). Through its association with microclimate, net radiation and energy
91 exchange (Coll et al., 2009; Sobrino et al., 2006; Voogt and Oke, 1998; Weng, 2009; Zhou and
92 Wang, 2011), LST is a major land surface parameter that also influences habitat quality and
93 thus the distribution of plants and animals and biodiversity.

94

95 The replacement of natural vegetation also changes evapotranspiration (ET) (Boisier et al.,
96 2014). ~~In case~~ When ET ~~is~~ decreases, surface temperatures and fluxes of sensible heat (H)
97 increase. ~~On the other hand, when~~ Vice versa when ET increases, the increased LE fluxes lower
98 surface temperatures and decrease H fluxes (Mahmood et al., 2014). Vegetation structure as
99 reflected by parameters such as the Normalized Difference Vegetation Index (NDVI), Leaf
100 Area Index (LAI) and vegetation height is in this respect an important determinant of the
101 resistances or conductivities to heat, moisture, and momentum transfer between the canopy and
102 the atmosphere (Bright et al., 2015) facilitating the amounts/ratios of sensible heat to water
103 vapour dissipation away from the surface (Hoffmann and Jackson, 2000).

104

105 Surface albedo, surface temperature, surface emissivity, and indirectly LAI and NDVI are
106 interconnected through the surface radiation balance. When the land surface is changed,
107 feedback mechanisms involving these biophysical variables control the radiation balance and
108 the surface temperature.

109 To understand the effects of land cover changes on LST, the associated biophysical variables
110 must be evaluated. This can be done through the surface radiation budget and energy
111 partitioning which unites these biophysical variables directly or indirectly: albedo as direct
112 determinant of the net solar radiation, NDVI as a vegetation parameter determining the
113 emissivity, which in turn determines the amount of reflected and emitted longwave radiation,
114 LST directly affecting the amount of emitted longwave radiation from the surface and ET,
115 [which](#) [affectsing](#) the amount of energy that is used for surface cooling via evaporating of water.

116
117 The effect of land cover change on LST is dependent on the scale, location, direction and type
118 of the change (Longobardi et al., 2016). Several studies showed an increase of the LST after
119 forest ~~were converted: in China to~~ built-up areas and agricultural land (Zhou and Wang,
120 2011); and ~~to~~ crop land and pasture lands (Peng et al., 2014). [in China](#). Similar findings were
121 reported for South American ecosystems: low vegetation such as grasslands in Argentina were
122 warmer than tall tree vegetation (Nosetto et al., 2005). In Brazil, the surface temperature
123 increased after the conversion of natural Cerrado vegetation (a savanna ecosystem) into
124 crop/pasture (Loarie et al., 2011a). Similar effects were also shown for other South American
125 biomes (Salazar et al., 2016). In a global analysis, Li et al. (2015) showed that the cooling of
126 forests is moderate at mid latitudes and that Northern boreal forests are even warmer, an
127 indication that the effect of land cover change on LST varies with the location of the land cover
128 change (Longobardi et al., 2016). Similar studies on the Indonesian Islands are lacking but
129 increases in surface temperature are expected as an effect of the expansion of oil palm and cash
130 crop land in the recent decades.

131

132 Measuring changes in LST is critical for understanding the effects of land cover changes, but
133 challenging. LST can be monitored with LST products retrieved from thermal infrared (TIR)
134 remote sensing data e.g. the use of the thermal bands of the Moderate Resolution Imaging
135 Spectrometer (MODIS) onboard the Terra and Aqua satellite (Sobrino et al., 2008), the thermal
136 band of the Thematic Mapper (TM) onboard the LANDSAT-5 platform (Sobrino et al., 2004,
137 2008) or Enhanced Thematic Mapper (ETM+) onboard the LANDSAT-7 platform. The
138 advantage of MODIS data is the availability of readily processed products at high temporal
139 resolution (daily) at medium (250 – 500 m) to coarse spatial resolution (1000 – 5000 m) scale;
140 MODIS LST product (MOD11A1/MYD11A1) for example is provided at a daily temporal
141 resolution with a spatial resolution of 1 km. Landsat data are provided at a higher spatial
142 resolution (30 m), but its temporal resolution is however limited to 16 days and the retrieval of
143 LST requires the correction of the satellite observed radiances for atmospheric absorption and
144 emission (Coll et al., 2009). Besides LST, the connected biophysical variables of the energy
145 and radiation budget can be derived from the visible and near-infrared (VIS-NIR) bands of
146 either MODIS or Landsat, making integrated monitoring of the biophysical variables related to
147 changing land surface possible. In Indonesia, a large proportion of the land use changes is
148 driven by small-holders (Dislich et al. 2016), thus a combination of Landsat (for a fine spatial
149 resolution) and MODIS (for temporal developments) seems desirable.

150

151 The modification of the physical properties of the land surface influences climate/local
152 microclimatic conditions via biogeochemical and biophysical processes. Therefore, given
153 Indonesia's history of large scale agricultural land conversion and governmental plans to
154 substantially expand the oil palm production, it is important to study the effect of the expansion
155 of cash crop areas on the biophysical environment, especially on LST as a key land surface
156 parameter. These effects have been poorly studied in this region and according to our

157 knowledge this is the first study to quantify the effects of land use change on LST in Indonesia
158 We focus on the province of Jambi / Sumatra as it experienced a large land transformation
159 towards oil palm and other cash crops such as rubber plantations in the past and it may serve as
160 an example of future changes in other regions.

161
162 Our main objective is to quantify the differences in LST across different land cover types and
163 to assess the impact of cash crop expansion on the surface temperature of Jambi province (on
164 Sumatra / Indonesia) in the past decades. With this study we aim to (1) evaluate the use of
165 Landsat and MODIS satellite data as sources for a reliable estimation of the surface temperature
166 in a tropical region with limited satellite data coverage by comparing the surface temperatures
167 retrieved from both satellite sources to each other and against ground observations, (2) to
168 quantify the LST variability across different land cover types and (3) to assess the long term
169 effects of land transformation on the surface temperature against the background of climatic
170 changes and (4) to identify the mechanisms that explain changes of the surface temperature
171 through changes in other biophysical variables. In this study we compare the surface
172 temperatures of different land cover types that replace forests (i.e. oil palm, rubber and acacia
173 plantations, clear cut land and urban areas) using high resolution Landsat and medium
174 resolution MODIS satellite data and discuss the differences by taking into account other
175 biophysical variables such as the albedo, NDVI and evapotranspiration (ET).

176

177 **2 Materials and methods**

178

179 **2.1 Study area**

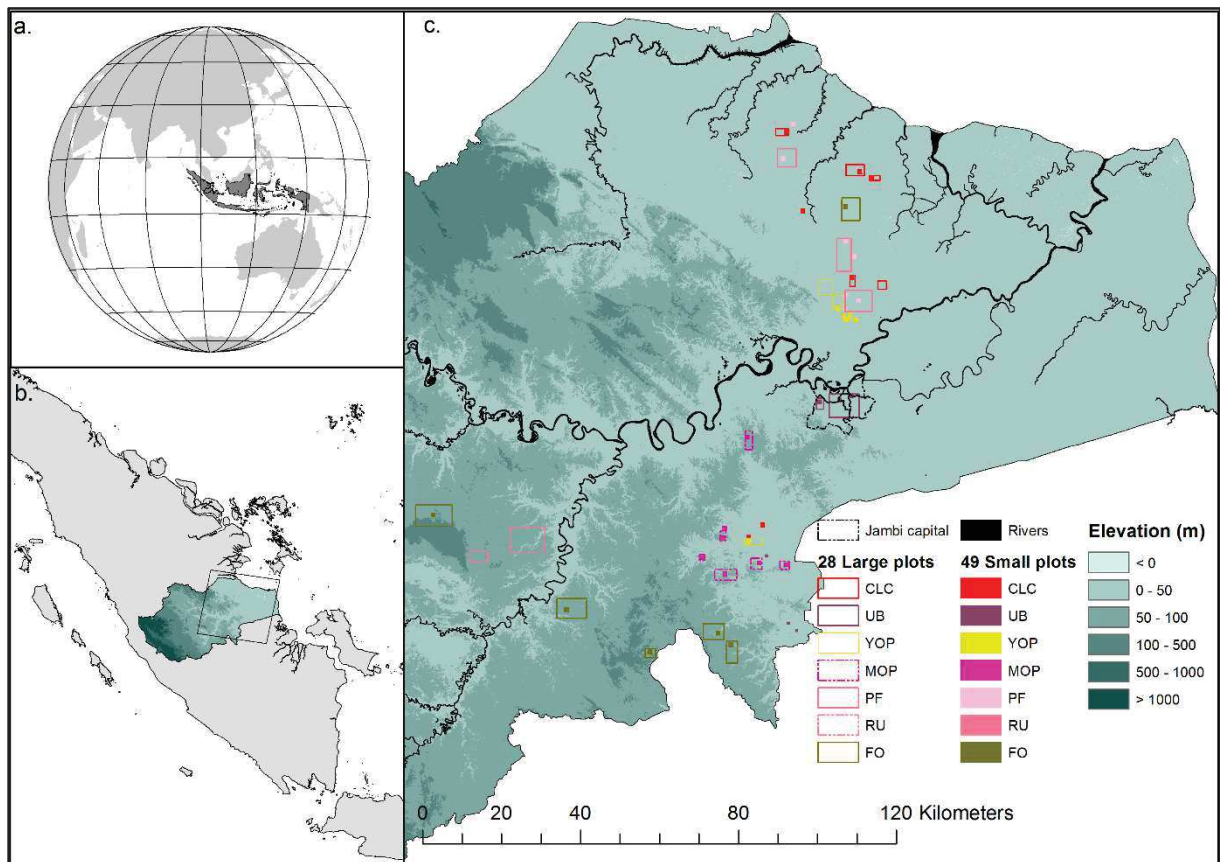
180

181 The study was carried out in the lowlands (approx. 25 000 km²) of the Jambi province (total
182 area 50 160 km²) on Sumatra, Indonesia, between latitudes 0°30'S and 2°30'S and longitudes

183 101°E and 104°30'E (Fig. 1). This region has undergone large land transformation towards oil
184 palm and rubber plantation over the past decades and thus may serve as an example of expected
185 changes in other regions of Indonesia (Drescher et al. 2016). The area has a humid tropical
186 climate with a mean annual temperature of 26.7 ± 0.2 °C (1991 – 2011, annual mean \pm SD of
187 the annual mean), with little intra-annual variation. Mean annual precipitation was 2235 ± 381
188 mm and a dry season with less than 120 mm monthly precipitation usually occurred between
189 June and September (Drescher et al., 2016). Previously logged rainforests in the Jambi province
190 have been converted to intensively managed agro-industrial production zones as well as into
191 smallholder farms to grow for cash crops of tree of rubber (*Hevea brasiliensis*) and oil palm
192 (*Elaeis guineensis*) or fast-growing tree species such as *Acacia mangium* for pulp production
193 ~~Details about the study area can be found in~~ (Drescher et al., 2016). The area cultivated with
194 oil palm grew faster than the area cultivated with rubber plantations between 1990 and 2011
195 (Clough et al. 2016).

196
197 For this study, we used two data sets of different plot sizes. For the first data set, we delineated
198 28 large plots (ranging from 4 to 84 km²) of 7 different land cover types (Forest (FO), Rubber
199 (RU), Acacia Plantation Forest (PF), Young oil palm plantation (YOP), Mature Oil Palm
200 Plantation (MOP), Urban area (UB) and ~~Clear-Cut~~Clear-Cut areas (CLC)) (Fig. 1). The
201 delineation was based on visual interpretation in combination with information from field work,
202 which was carried out between October – December 2013. The large size of the plots was
203 necessary to make a comparison between MODIS and Landsat images (see section satellite
204 data). For the second data set, we selected 49 smaller plots within and outside these 28 large
205 plots ~~49 smaller plots~~ (between 50 × 50 m and 1000 × 1000 m) (Fig. 1) which allowed us to
206 increase the number of plots to use when analysing Landsat images. These small plots were
207 used to extract surface temperature (LST), Normalized Difference Vegetation Index (NDVI),

208 albedo (α) and evapotranspiration (ET) from a high resolution Landsat satellite image (see
 209 section satellite data) for the 7 different land cover types of interest.



210
 211 **Fig. 1** Geographic location of the study area. Jambi province on the Sumatran Island of
 212 Indonesia (Figs. 1a and 1b). The background of the map (Fig. 1c) is a digital elevation model,
 213 showing that the plots are located in the lowlands of the Jambi province. The large rectangles
 214 are the 28 different land cover types (Forest, Young and Mature Oil palm, Rubber, Urban area,
 215 Acacia Plantation Forest and ~~Clear-Cut~~ Clear-Cut land), the small squares are the locations of
 216 the 49 small plots of the 7 different land cover types. Abbreviations: CLC = Clear-cut land,
 217 UB = Urban area, YOP = Young oil palm plantation, MOP = Mature Oil Palm plantation, PF
 218 = Acacia plantation forest, RU = Rubber plantation, FO = Forest.

219
 220 **2.2 Meteorological data**
 221

222 Air temperature and relative air humidity were measured at four reference meteorological
 223 stations located in open areas within the area of study (Drescher et al., 2016), with

224 thermohygrometers (type 1.1025.55.000, Thies Clima, Göttingen, Germany) placed at 2m
225 height. Measurements were taken every 15 s and then averaged and stored in a DL16 Pro data
226 logger (Thies Clima, Göttingen, Germany) as 10 min mean, from February 2013 to December
227 2015. We used the air temperature from the meteorological stations to compare to MODIS air
228 temperatures (MOD07_L2). The relative air humidity was used as an input parameter for
229 NASA's online atmospheric correction (ATCOR) parameter tool to derive parameters to correct
230 Landsat thermal band for atmospheric effects (see Satellite data). We also used air temperature
231 and relative humidity from two eddy covariance flux towers located in the study area (Mejjide
232 et al., 2017) one in a young oil palm plantation (two years old, S 01°50.127', E 103°17.737'),
233 and the other one in a mature oil palm plantation (twelve years old, S 01°41.584', E
234 103°23.484'). At these flux towers, air temperature and relative humidity were measured above
235 the canopy respectively with the same instruments as in the reference meteorological stations
236 (see Mejjide et al. (2017), for description of methodology). In the flux tower located in the
237 mature oil palm plantation, we also measured surface canopy temperature between August 2014
238 and December 2015, which was compared to MODIS LST estimates from the same period.
239 Measurements of canopy temperature were performed with two infrared sensors (IR100)
240 connected to a data logger, (CR3000) both from Campbell Scientific Inc. (Logan, USA). For a
241 regional coverage we used ERA Interim daily air temperature grids
242 (<http://apps.ecmwf.int/datasets/data/interim-full-daily/levtype=sfc/>; (Dee et al., 2011) from
243 2000 – 2015 at 0.125 degrees resolution to study the annual air temperature trend in this period.

244

245 **2.3 Satellite data**

246

247 A Landsat 7 ETM+ VIS/TIR 30 m resolution surface reflectance image with low cloud cover,
248 acquired at 10:13 hours (local time) on 19 June 2013 covering the lowland area of the Jambi
249 province (path 125, row 61) was used in this study. Like all Landsat 7 ETM+ images acquired

250 after 31 ~~may~~May 2003, the image we used was affected by a scan line error causing a data loss
251 of about 22% (http://landsat.usgs.gov/products_slcutoffbackground.php). Most selected plots
252 were located in the center of the image and thus not affected by the data loss, e.g. the forest
253 plots located at the edges of the scan line error zone faced minimal data loss because they were
254 large enough.

255 We also downloaded the tile h28v09 of the MODIS Terra (MOD) and Aqua (MYD) daily 1km
256 Land Surface Temperature and Emissivity products (MOD11A1 and MYD11A1 Collection-5)
257 and MODIS 16-days 500 m Vegetation Indices NDVI/EVI product (MOD13A1 Collection-5)
258 from 05 March 2000 till 31 December 2015 for Terra data and from 8 July 2002 till 31
259 December 2015 for Aqua data. We downloaded other supporting satellite data such as the
260 MODIS Atmospheric Profile product (MOD07_L2) and the MODIS Geolocation product
261 (MOD03). All MODIS data were reprojected to WGS84, UTM zone 48 South using the MODIS
262 Reprojection Tool (MRT). The quality of the MODIS data was checked using the provided
263 quality flags and only pixels with the highest quality flag were used in the analysis.

264

265 **2.4 Retrieval of biophysical variables from Landsat 7 ETM+ VIS/TIR images**

266

267

- 268 • *NDVI*

269

270 NDVI was derived using the reflectances corrected for atmospheric effects in the red (ρ_{RED} ,
271 band 3 Landsat 7 ETM+) and near infrared (ρ_{NIR} , band 4 Landsat 7 ETM+) bands, with:

272

273

$$274 \quad NDVI = \frac{\rho_{NIR} - \rho_{RED}}{\rho_{NIR} + \rho_{RED}} \quad (1)$$

275

276 • *Surface albedo*

277

278 The surface albedo (α) was computed using the equation of Liang (2000) for estimating
279 broadband albedo from Landsat surface reflectance bands, with:

280

$$281 \alpha = 0.3141 \rho_1 + 0.1607 \rho_3 + 0.369 \rho_4 + 0.1160 \rho_5 + 0.0456 \rho_7 - 0.0057 \quad (2)$$

282

283 where $\rho_1, \rho_3, \rho_4, \rho_5$ and ρ_7 are the Landsat 7 ETM+ surface reflectance bands (corrected for
284 atmospheric effects).

285

286 • *Surface temperature (LST)*

287

288 LST was derived following the method proposed by Bastiaanssen (2000), Bastiaanssen et al.
289 (1998a), Coll et al. (2010) and Wukelic et al. (1989) for computing the surface temperature
290 from the thermal infrared band (TIR, band 6) of Landsat (Supporting information, S1). The
291 thermal infrared band (TIR, band 6) was first converted to thermal radiance (L_6 , $W/m^2/sr/\mu m$)
292 and then to atmospherically corrected thermal radiance (R_c , $W/m^2/sr/\mu m$) following the method
293 described by Wukelic et al. (1989) and Coll et al. (2010), and using the atmospheric parameters
294 obtained on NASA's online Atmospheric Correction Calculator (Barsi et al., 2003, 2005)
295 (supporting information, S2). The surface temperature (LST, $^{\circ}K$) was computed through the
296 following equation similar to the Planck equation, as in Coll et al. (2010) and Wukelic et al.
297 (1989):

298

299
$$LST = \frac{k_2}{\ln\left(\frac{\epsilon_{NB} \cdot k_1}{R_c} + 1\right)}$$
 (3)

300

301 where ϵ_{NB} is the emissivity of the surface obtained from the NDVI (Supporting information,
 302 Table S1), k_1 (= 666.09 mW/cm²/sr/μm) and k_2 (= 1282.71 °K) are sensor constants for
 303 converting the thermal radiance obtained from band 6 of Landsat 7 to surface temperature.

304 The surface temperature derived from Landsat thermal band was compared with a MODIS LST
 305 product that was acquired on the same day at 10:30 am local time. For this, the Landsat LST
 306 image was resampled to MODIS resolution to enable a pixel to pixel comparison, followed by
 307 extracting the average LST of 7 land cover types using the data set containing the large
 308 delineated plots (Fig. 1).

309

310 • *Evapotranspiration (ET)*

311

312 Based on the Surface Energy Balance Algorithm for Land (SEBAL) (Bastiaanssen, 2000;
 313 Bastiaanssen et al., 1998a, 1998b) we estimated ET (mm/hr) from latent heat fluxes (LE, W/m²)
 314 which were computed as the residual from sensible (H, W/m²) and ground (G, W/m²) heat
 315 fluxes subtracted from net radiation (R_n, W/m²) as:

316

317
$$LE = R_n - G - H$$
 (4)

318

319 We calculated R_n as the sum of incoming shortwave and longwave radiation, minus the
 320 reflected shortwave and longwave radiation and the emitted longwave radiation (equation 5).

321 The surface albedo, surface emissivity and surface temperature determine the amounts of
 322 incoming and reflected radiation:

323

324 $R_n = (1 - \alpha) S_{d\downarrow} + \epsilon_a \sigma T_a^4 - (1 - \epsilon_0) \epsilon_a \sigma T_a^4 - \epsilon_0 \sigma LST^4$ (5)

325

326 Where $S_{d\downarrow}$ is the incoming shortwave solar radiation (W/m^2) at the surface; α is the surface
 327 albedo (equation 2); ϵ_0 is the surface emissivity (-); ϵ_a is the atmospheric emissivity (-); σ is the
 328 Stephan-Boltzmann constant ($5.67 \times 10^{-8} W/m^2/K^4$); LST is the surface temperature (K,
 329 equation 3); T_a is the near surface air temperature (K). The surface emissivity (ϵ_0) is derived
 330 from the NDVI and is described in the supporting information (Table S1). The average
 331 atmospheric emissivity (ϵ_a) is estimated with the model of Idso and Jackson, (1969):

332

333 $\epsilon_a = 1 - 0.26 \cdot \exp \{(-7.77 \times 10^{-4}) \cdot (273.15 - T_a)^2\}$ (6)

334

335 Ground heat fluxes (G , W/m^2) were derived as a fraction of R_n from an empirical relationship
 336 between LST, α , and NDVI (Bastiaanssen, 2000) as:

337

338 $G = R_n \cdot \frac{LST - 273.15}{\alpha} \cdot (0.0038\alpha + 0.0074\alpha^2) \cdot (1 - 0.98NDVI^4)$ (7)

339

340 In SEBAL Sensible heat flux (H , W/m^2) was calculated as:

341

342 $H = \rho C_p \frac{\Delta T}{r_{ah}} = \rho C_p \frac{a LST + b}{r_{ah}}$ (8)

343

344 Where ρ is the air density ($1.16 kg/m^3$); C_p is the specific heat of air at constant pressure (1004
 345 $J/kg/K$); r_{ah} is the aerodynamic resistance to heat transport ($s m^{-1}$); a and b are regression
 346 coefficients which are determined by a hot extreme pixel (where $LE = 0$ and H is maximum)
 347 and a cold extreme pixel (where $H = 0$ and LE is maximum). The aerodynamic resistance to
 348 heat transport, r_{ah} , is calculated through an iterative process with air temperature measured at 2

349 m as input. SEBAL is described in Bastiaanssen (2000) and Bastiaanssen et al. (1998a, 1998b).
350 The application of SEBAL in this research is briefly described in the supporting information
351 (S3: ET from satellite images).

352

353 **2.5 Local short term differences between different land cover types**

354

355 From the created LST, NDVI, Albedo and ET images we extracted the average values of the
356 different land cover classes. For this we used the dataset containing the small 49 delineated
357 plots covering 7 different land cover types (Fig. 1). The average effect of land transformation,
358 i.e. the change from forest to another non-forest land cover type, on the surface temperature
359 was evaluated as (cf. Li et al. (2015)) :

360

$$361 \quad \Delta LST = LST_{\text{non-forest}} - LST_{\text{forest}} \quad (39)$$

362

363 A negative ΔLST indicates a cooling effect and positive ΔLST indicates a warming effect of
364 the non-forest vegetation compared to forest. The same procedure was applied in evaluating the
365 effect of land transformation on the NDVI, albedo and ET.

366

367 **2.6 Effects of land cover change on the provincial surface temperature in the past decades**

368

369 To analyse the ~~long-term~~[long-term](#) effects on the provincial scale we used the MODIS daily
370 LST time series (MOD11A1 and MYD11A1) from 2000 – 2015. MOD11A1 provides LST for
371 two times of the day: 10:30 am and 10:30 pm and we used the times series between 2000 and
372 2015. MYD11A1 provides LST for 1:30 am and 1:30 pm and is available from 8 July 2002; we
373 used complete years in our analysis and therefore used the MYD11A1 time series from 2003 –
374 2015. We calculated the mean annual LST at four different times of the day (10:30 am, 1:30

375 pm, 10:30 pm and 1:30 am) between 2000 and 2015 for the lowland of the Jambi from the
 376 MODIS daily LST time series (MOD11A1 and MYD11A1). To do so (1) we calculated for
 377 each pixel the average LST pixel value using only the best quality pixels for every year; (2)
 378 from these pixels we made a composite image (n = 16, one for each year) for the province and
 379 (3) from each composite image we calculated the mean annual lowland provincial temperature
 380 as the average of all the pixels that are enclosed by a zone delineating the lowland of the Jambi
 381 province. We performed the same analysis with the MODIS 16-day NDVI product (2000 –
 382 2015) and the ERA daily temperature grid (2000 – 2015) to compare the annual trends of LST,
 383 NDVI and air temperature of the province. The average provincial LST and NDVI were
 384 compared to the mean LST and NDVI of a selected forest that remained undisturbed forest
 385 during the 2000 – 2015 period.

386

387 2.7 Statistical analysis

388

389 For comparison of the Landsat derived LST and the MODIS LST we analyzed the statistical
 390 relationships with the coefficient of determination (R^2), the root mean square error (RMSE),
 391 the mean absolute error (MAE) and the bias (Bias):

$$392 \quad \text{RMSE} = \sqrt{\frac{\sum_{i=1}^N (E_i - O_i)^2}{N}} \quad (910)$$

393

$$394 \quad \text{Bias} = \frac{\sum_{i=1}^N (E_i - O_i)}{N}$$

$$395 \quad (1011)$$

396

$$397 \quad \text{MAE} = \frac{\sum_{i=1}^N |E_i - O_i|}{N}$$

$$398 \quad (1112)$$

399

400 Where O_i is MODIS LST, E_i is the Landsat surface temperature, and N is the number of pixels
401 compared. Model type 2 linear regression was applied for fitting the relation between MODIS
402 LST and Landsat LST.

403 We tested the relation between the biophysical variables LST (or L6 and Rc, both as pre- or
404 intermediate products before obtaining LST), albedo (α), NDVI and ET with correlation
405 analysis and a multiple linear regression was applied to analyse the effects of the biophysical
406 variables on the LST. We used the model: $LST \text{ (or Rc or L6)} \sim \alpha + NDVI + ET$, and used R^2
407 and standardized β -coefficients to evaluate the strength of the biophysical variables in
408 predicting the LST.

409

410 **3 Results**

411

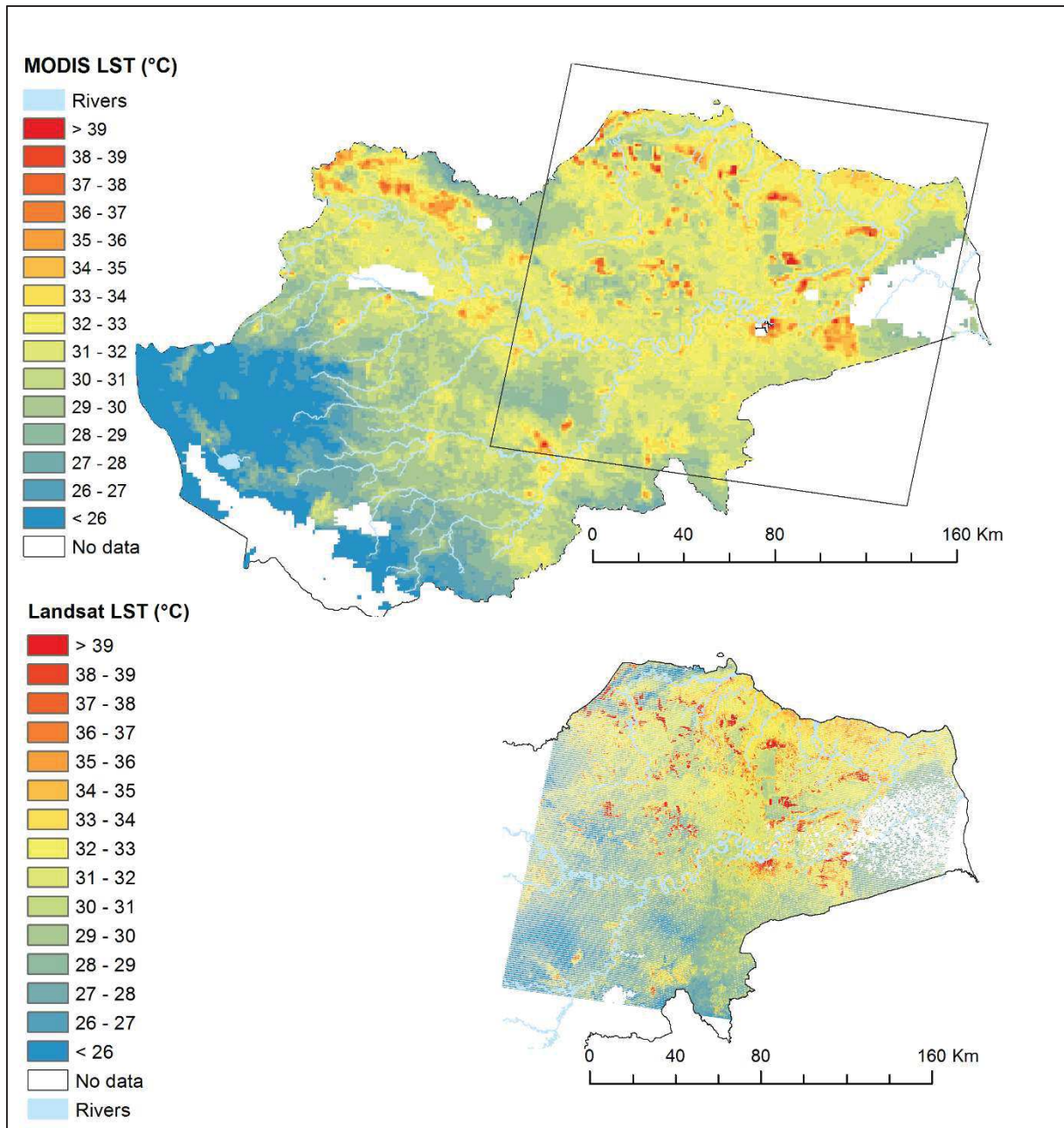
412 **3.1 Landsat LST compared to MODIS LST**

413

414 Landsat and MODIS images showed similar spatial patterns of LST (Fig. 2). In both images the
415 hot areas (red) correspond to the known clear cut areas, urban areas or other sparsely vegetated
416 areas, the cooler areas (blue) correspond to vegetated areas such as forest, plantation forests and
417 mature oil palm plantations. The coarse resolution scale of MODIS (1000 m for LST) allows a
418 large regional coverage of the study area but does not allow to retrieve detailed information on
419 small patches (smaller than 1 km²). On the other hand, Landsat 7 image allows a detailed study
420 of patches that are small enough (as small as 30 x 30 m²), but is affected by the scan line error
421 causing data loss at the edges of the image. In both MODIS and Landsat images clouds and
422 cloud shadows were removed and therefore lead to data gaps in the images.

423

424



426

427

428

429

430

431

432

433

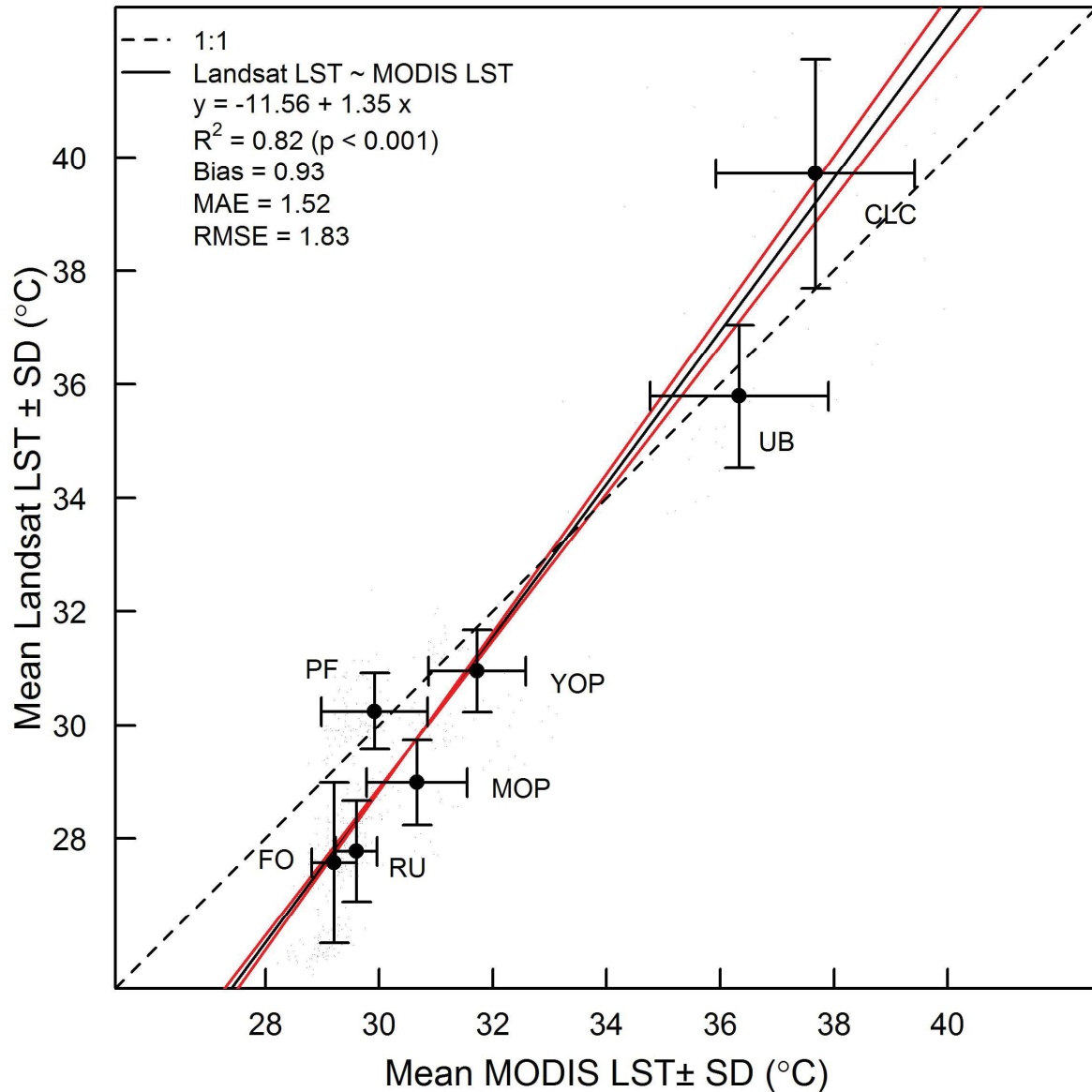
434

435

Fig. 2 MODIS LST image (top) compared with Landsat LST image (bottom). Cloud cover and cloud shadow cover resulted in data gaps (No data). The difference in acquisition time between the images is 15 minutes. The square in the MODIS image is the area that is covered by the Landsat tile (path 125, row 61). Both satellite images were acquired on 19 June 2013.

Landsat derived LST correlated well with MODIS LST ($R^2 = 0.82$; $p < 0.001$; Fig. 3) with a RMSE of 1.83°C . The 7 land cover types had distinctive LSTs and the observed differences

436 between these land cover types were consistent in both images. The non-vegetated surfaces
437 (Clear cut land (CLC) and Urban areas (UB)) had higher surface temperatures than the
438 vegetated surface types (FO, YOP, MOP, PF and RU). Clear cut land had the highest surface
439 temperature of all compared land cover types, followed by urban areas whereas the vegetated
440 land cover types had lower surface temperatures: $LST_{CLC} (39.71 \pm 2.01 \text{ }^\circ\text{C}) > LST_{UB} (35.79 \pm$
441 $1.26 \text{ }^\circ\text{C}) > LST_{YOP} (30.95 \pm 0.72 \text{ }^\circ\text{C}) > LST_{PF} (30.25 \pm 0.67 \text{ }^\circ\text{C}) > LST_{MOP} (28.98 \pm 0.75 \text{ }^\circ\text{C})$
442 $> LST_{RU} (27.78 \pm 0.89 \text{ }^\circ\text{C}) > LST_{FO} (27.57 \pm 1.41 \text{ }^\circ\text{C})$ (Landsat LST, Fig. 3). The same trend
443 was derived from the MODIS image but with higher surface temperatures, except for CLC:
444 $LST_{CLC} (37.67 \pm 1.75 \text{ }^\circ\text{C}) > LST_{UB} (36.33 \pm 1.57 \text{ }^\circ\text{C}) > LST_{YOP} (31.73 \pm 0.85 \text{ }^\circ\text{C}) > LST_{MOP}$
445 $(30.67 \pm 0.88 \text{ }^\circ\text{C}) > LST_{PF} (29.92 \pm 0.93 \text{ }^\circ\text{C}) > LST_{RU} (29.60 \pm 0.36 \text{ }^\circ\text{C}) > LST_{FO} (29.21 \pm 0.40$
446 $^\circ\text{C})$ (MODIS LST, Fig. 3).



447
 448 **Fig. 3** Average surface temperature (LST) and standard deviation (SD) of 7 land cover types
 449 derived from Landsat thermal image compared with the mean and SD of MODIS LST.
 450 CLC = Clear cut land, UB = Urban areas, YOP = young oil palm plantation, PF = Acacia
 451 Plantation Forest, MOP = Mature Oil palm plantation, FO = Forest, RU = Rubber plantation.
 452 The dashed line is the theoretical 1:1 line, the solid lines are the Linear Model type 2 regression
 453 line (black) and the confidence limits of the regression line (red). Landsat and MODIS images
 454 were acquired on 19 June 2013, Landsat at 10:13 am local time, MODIS at 10:30 am local time.
 455 Landsat pixels (30 m) were resampled to MODIS pixel resolution (926 m) to make a pixel to

456 pixel comparison between the two sources possible. RMSE is the root mean squared error, MAE
457 is the mean absolute error.

458

459 **3.2 Local short term differences between different land cover types**

460

461 The Δ LST between RU, MOP, PF, YOP, UB and CLC land cover types and FO were all
462 positive, meaning that all other land cover types were warmer than forests (Fig. 4a & Supporting
463 Information S4 and S5). RU and MOP were 0.4 ± 1.5 °C and 0.8 ± 1.2 °C warmer than forest,
464 respectively. PF and YOP were much warmer than forests (Δ LST_{PF-FO} = 2.3 ± 1.1 °C, Δ LST_{YOP}
465 _{-FO} = 6.0 ± 1.9 °C). The largest Δ LSTs were between forest and the non-vegetated land cover
466 types, i.e. UB (Δ LST = 8.5 ± 2.1 °C) and CLC (Δ LST = 10.9 ± 2.6 °C). The LST differences
467 were significant ($p < 0.05$, post-hoc Tukey's HSD test), except between RU and FO ($p = 0.78$,
468 post-hoc Tukey's HSD test (Supporting Information S6, Table S6.1 & table S6.2).

469

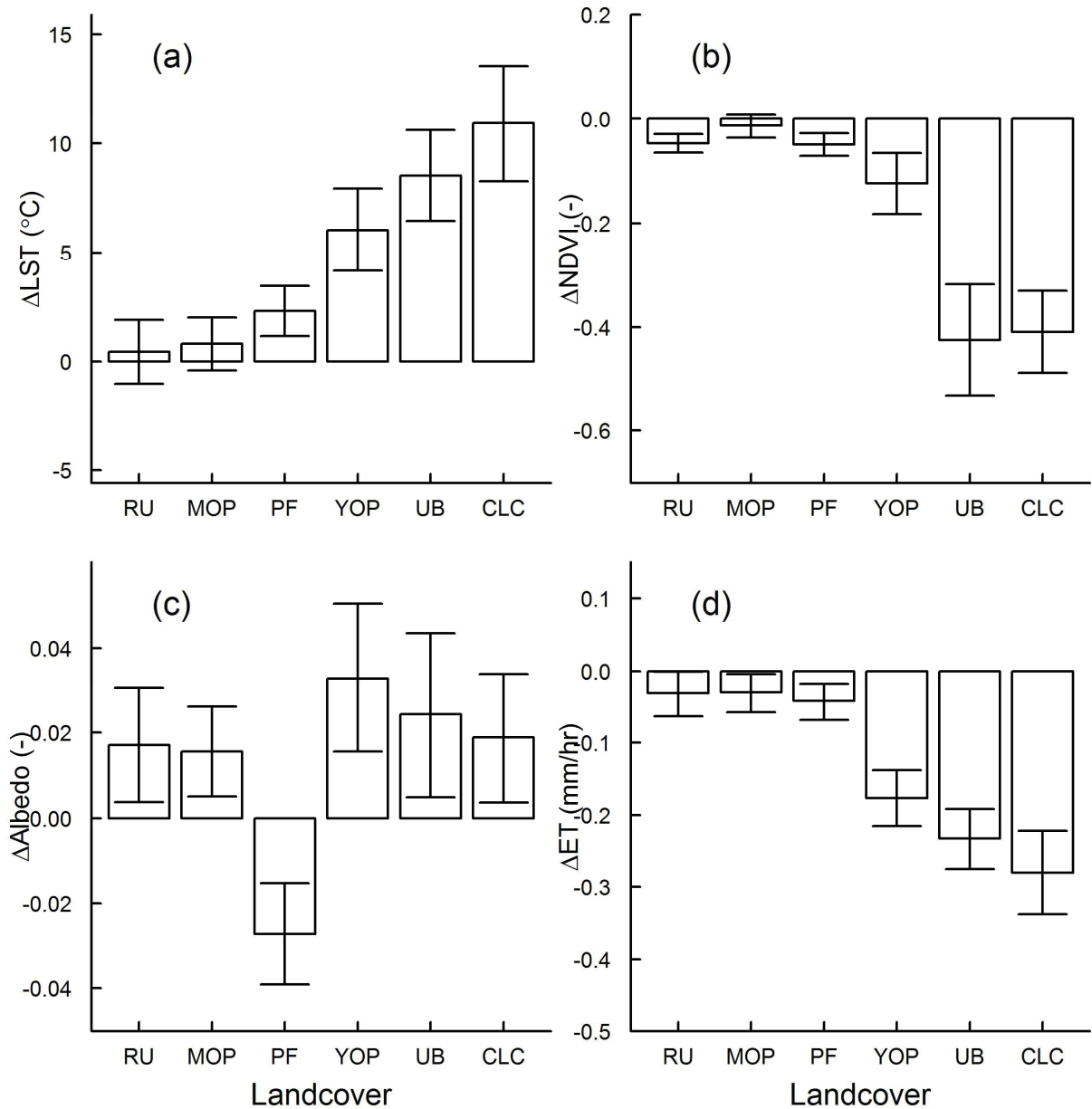
470 Similar differences were found for the Δ NDVI between forest and other land covers (Fig. 4b).
471 The negative Δ NDVI indicates that the non-forest land cover types had lower NDVI than forest.
472 Δ NDVI between FO and RU, MOP, PF and YOP were small (between -0.01 ± 0.02
473 (Δ NDVI_{MOP-FO}) and -0.12 ± 0.06 (Δ NDVI_{YOP-FO}). The largest Δ NDVIs were between forest
474 and the non-vegetated land cover types, i.e. UB and CLC (Δ NDVI = -0.42 ± 0.11 and -0.41
475 ± 0.08 , respectively). All Δ NDVIs were significant ($p < 0.05$, post-hoc Tukey's HSD test).

476

477 The difference in albedo (Δ Albedo) between forest and the other land covers was very small
478 (Fig. 4c), with Δ Albedo values between -0.03 ± 0.01 (Δ Albedo_{PF-FO}) and 0.03 ± 0.02
479 (Δ Albedo_{YOP-FO}). These differences were significant ($p < 0.05$, post-hoc Tukey's HSD test).
480 PF had a lower albedo than forest (Δ Albedo_{PF-FO} = -0.03 ± 0.01), while the other land cover
481 types had a higher albedo than forest.

482
483
484
485
486
487
488
489
490
491
492

~~The SEBAL based LE estimates were within the variability range of LE measurements from eddy covariance techniques under similar meteorological conditions (see SI 3).~~ All land covers had lower ET than forest. RU, MOP and PF had slightly lower ET than FO ($\Delta ET_{RU-FO} = -0.03 \pm 0.04$, $\Delta ET_{MOP-FO} = -0.03 \pm 0.03$ mm/hr, $\Delta ET_{PF-FO} = -0.04 \pm 0.03$ mm/hr) (Fig. 4d). YOP, UB and CLC had much lower ET values than forests: $\Delta ET_{YOP-FO} = -0.18 \pm 0.04$ mm/hr, $\Delta ET_{UB-FO} = -0.23 \pm 0.04$ mm/hr, $\Delta ET_{CLC-FO} = -0.26 \pm 0.06$ mm/hr). The ΔET s were significant ($p < 0.05$, post-hoc Tukey's HSD test). The SEBAL based LE estimates were within the variability range of LE measurements from eddy covariance measurements techniques under similar meteorological conditions (see SI 3).



493
 494 **Fig. 4** Differences (mean \pm SD) in surface temperature (Δ LST), normalized difference
 495 vegetation index (Δ NDVI), Albedo (Δ Albedo) and Evapotranspiration (Δ ET) between other
 496 land covers (RU, MOP, PF, YOP, UB and CLC) and forest (FO) in the Jambi province, derived
 497 from the Landsat LST image acquired on 19 June 2013 at 10:13 am local time.

498
 499 Albedo had the-a weakerrst influence on the LST ($\rho = 0.25$, $p < 0.05$) (Table 2) than NDVI and
 500 ET. As the thermal radiance band (L6) and the atmospherically corrected thermal band (Rc)
 501 were the basis for the LST calculation, the high correlation between L6 and NDVI ($\rho = -0.87$,

502 $p < 0.05$) and between L6 and ET ($\rho = -0.98$, $p < 0.05$) resulted in a high correlation between
 503 LST and NDVI ($\rho = -0.88$) and between LST and ET ($\rho = -0.98$). The analysis showed that
 504 albedo, NDVI and ET were all significant predictors of LST ($F_{(3, 41586)} = 1 \times 10^6$, $p < 0.05$). ET
 505 was the strongest predictor of LST (stand. $\beta = -1.11$, $p < 0.05$). Albedo (stand. $\beta = -0.19$, $p <$
 506 0.05 , resp.) and NDVI (stand. $\beta = -0.19$, $p < 0.05$) were weaker predictors of LST.

507

508 **Table 2** Statistical analysis between biophysical variables (albedo (α), NDVI and ET) and
 509 Spectral Radiance band (L6), corrected thermal band (Rc) and Landsat surface temperature
 510 (LST).

Model		ρ	R^2	β	Stand. β	Model fit (R^2)	F-statistics
L6 ~ α + NDVI + ET	α	0.26	0.05	-2.94	-0.19	0.99	F (3, 41586) = 1.10×106, ***
	NDVI	-0.87	0.10	0.23	0.11		
	ET	-0.98	1.13	-4.00	-1.16		
Rc ~ α + NDVI + ET	α	0.25	0.05	-4.88	-0.20	0.99	F (3, 41586) = 1.79×106, ***
	NDVI	-0.88	0.04	0.16	0.05		
	ET	-0.98	1.00	-6.21	-1.10		
LST ~ α + NDVI + ET	α	0.25	0.05	-34.01	-0.19	0.99	F(3, 41586) = 2.3×106, ***
	NDVI	-0.88	0.05	1.30	0.05		
	ET	-0.98	1.00	-43.53	-1.11		

511 ***: $p = 2 \times 10^{-16}$

512 LM: Multiple linear regression analysis between LST (or L6 or Rc) and 3 biophysical variables:
 513 Albedo (α), NDVI and ET. ρ = correlation coefficient; R^2 : R-squared of the components; β =
 514 regression coefficient of the component; stand. β = standardized β ; Model fit (R^2): overall model
 515 fit of the multiple linear regression. The values in brackets are for the analysis between the
 516 biophysical variables and the corrected thermal band (Rc).

517

518 A separate analysis (Table S6.3, Supporting information S6) showed that ET was a strong
 519 predictor of LST for each land cover type in this study and that NDVI and albedo were minor
 520 predictors of LST.

521

522 3.3 Effects of land-use change on the provincial surface temperature in the past decades

523

524 The average annual LST of the province was characterized by a fluctuating but increasing trend
525 during daytimes (Fig. 5a and 5b) between 2000 and 2015. The average morning LST (10:30
526 am) increased by 0.07 °C per year ($R^2 = 0.59$; $p < 0.0001$), the midday afternoon LST (13:30
527 local time) increased by 0.13 °C per year ($R^2 = 0.35$; $p = 0.02$) between 2003 and 2015. While
528 the daytime LST showed a clear increase, the night and evening LST (10:30 pm and 1:30 am,
529 Fig. 5c and 5d) trends were small showing a decrease of -0.02 °C ($R^2 = 0.29$; $p = 0.02$) and $-$
530 0.01 °C ($R^2 = 0.05$; $p = 0.51$) per year, respectively. The observed LST trends resulted in a total
531 LST increase of 1.05 °C and 1.56 °C in the morning (10:30 am) and afternoon (1:30 pm)
532 respectively and a total decrease of the province LST of 0.3 °C (10:30 pm) and 0.12 °C (1:30
533 am) at night over the ~~time~~ period from 2000 to 2015.

534

535 In order to separate the effect of land use change from global climate warming, we used a site
536 constantly covered by forest over that period (from the forest sites we used in this study) as a
537 reference- not directly affected by land cover changes. That site showed less changes in LST
538 than the entire province: -only the mean morning LST (10:30 am) had a significant but small
539 trend with an increase by 0.03 °C per year ($R^2 = 0.21$, $p < 0.05$) resulting in a total LST increase
540 of the province of 0.45 °C between 2000 and 2015 (Fig. 5a). This LST warming is much smaller
541 than the overall warming at provincial level of 1.05 °C. The LST time series at other times
542 showed no significant trends: the mean afternoon LST (1:30 pm) with -0.05 °C per year ($R^2 =$
543 0.01 , $p = 0.31$) (Fig. 5b), the night and evening LST with 0.01°C per year (Fig. 5c and 5d, $p =$
544 0.19 and $p = 0.65$, respectively).

545

546 The mean annual NDVI of the province decreased by 0.002 per year, which resulted in a total
547 NDVI decrease of 0.03 ($R^2 = 0.34$; $p = 0.01$; Fig. 5e). The NDVI of the forest showed a small

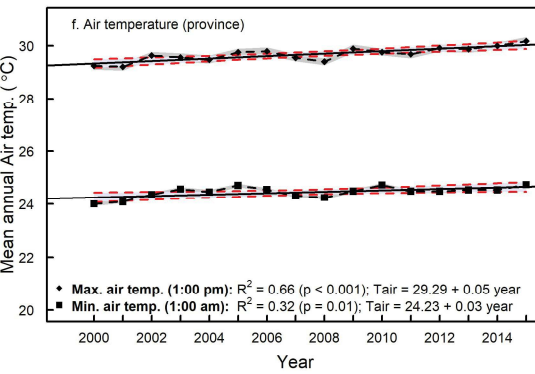
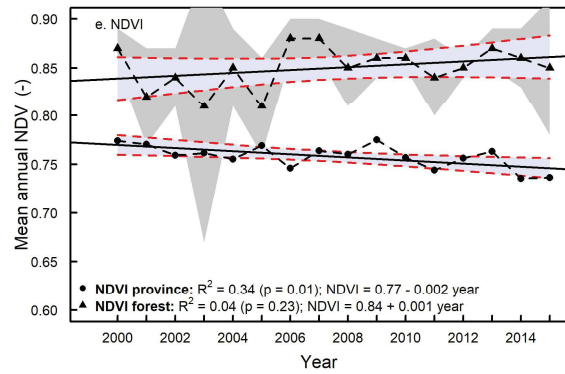
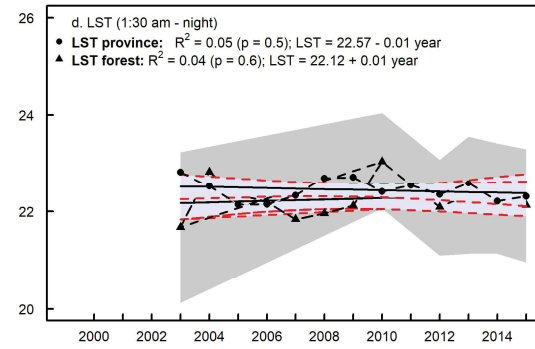
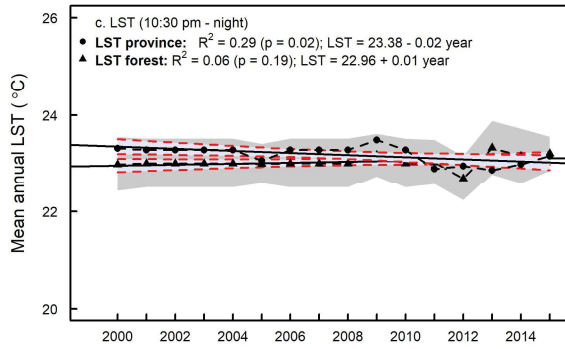
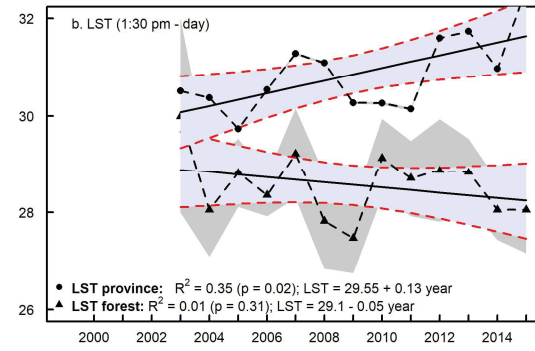
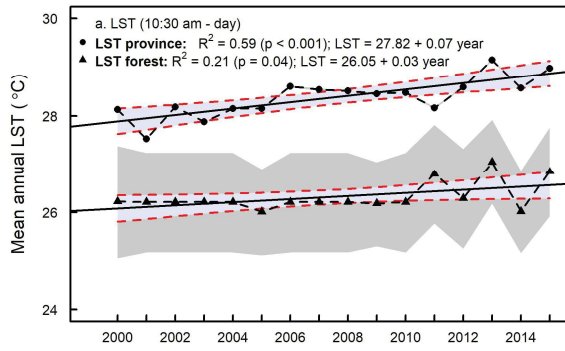
548 but not significant increase of 0.001 per year ($R^2 = 0.04$, $p = 0.23$) (Fig. 5e) fluctuating around
549 an NDVI of 0.84.

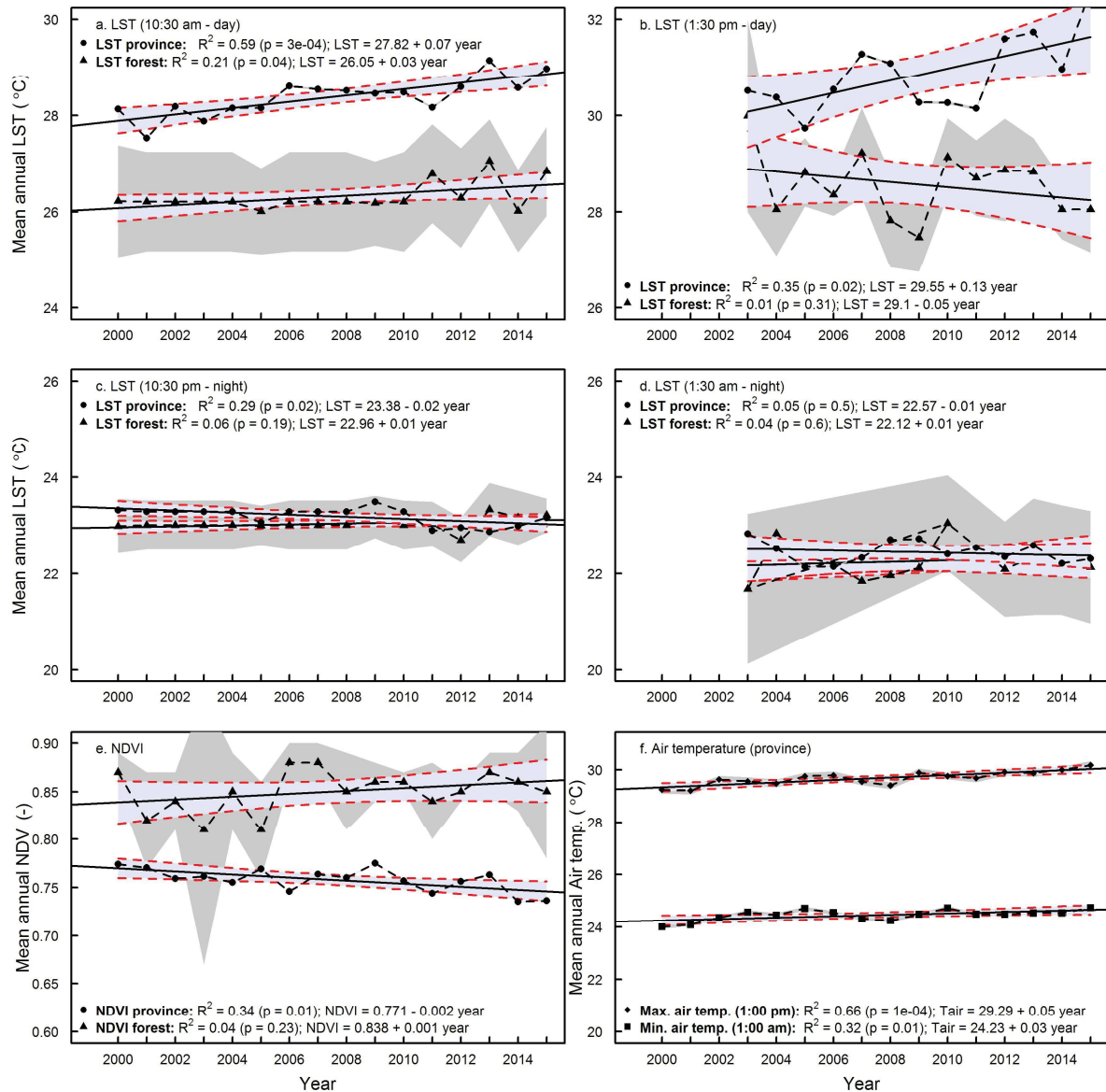
550

551 The mean annual midday air temperature (at 1:00 pm, local time, Fig. 5f) and the mean annual
552 night air temperature (at 1:00 am, local time) increased every year by 0.05 °C and 0.03 °C,

553 respectively resulting in a total air temperature increase of 0.75 °C ($R^2 = 0.66$, $p < 0.0001$) and

554 0.45 °C ($R^2 = 0.32$, $p = 0.014$) between 2000 and 2015 (Fig. 5f).





556

557 **Fig 5.** Mean annual LST (a – d), mean annual NDVI (e) and mean annual air temperature trends

558 (f) in the Jambi province between 2000 and 2015 derived from MODIS LST (5a. 10:30 am, 5b.

559 1:30 pm, 5c. 10:30 pm and 5d. 1:30 am, local time), MODIS NDVI and ERA Interim Daily air

560 temperature (1:00 am and 1:00 pm, local time) data sets respectively. Grey-shaded areas are the

561 confidence intervals of the means, blue-shaded areas are the confidence intervals of the

562 regression lines. MODIS LST time series for 1:30 pm and 1:30 am were available from the mid

563 of 2002; for this reason we used the complete years from 2003 till 2015.

564

565 **4 Discussion**

566

567 4.1 Landsat LST compared to MODIS LST

568

569 In our study we retrieved the surface temperature from a Landsat image and compared this with
570 MODIS LST. Our results showed a good agreement between both LSTs (Fig. 3), which is
571 comparable to other studies and thus gives confidence in our analysis. Bindhu et al. (2013)
572 found also a close relationship between MODIS LST and Landsat LST using the same
573 aggregation resampling technique as our method and found R^2 of 0.90, a slope of 0.90, and
574 an intercept of $25.8\text{ }^\circ\text{C}$ for LST, compared to our R^2 of 0.8, slope of 1.35 and intercept of $-$
575 $11.58\text{ }^\circ\text{C}$ (Fig. 3). Zhang and He (2013) validated Landsat LST with MODIS LST and also
576 found good agreements (RMSD $0.71 - 1.87\text{ }^\circ\text{C}$) between the two sensors, where we found a
577 RMSE of $1.71\text{ }^\circ\text{C}$. Nevertheless, there still are differences and slope versatility between the two
578 satellite sources. These differences are typically caused by differences between MODIS and
579 Landsat sensors in terms of (a) different sensor properties e.g. spatial and radiometric resolution
580 and sensor calibration; (b) geo-referencing and differences in atmospheric corrections (Li et al.,
581 2004); and (c) emissivity corrections i.e. the use of approximate equations to derive the
582 emissivity from the NDVI from Landsat's Red and NIR bands. Li et al. (2004) and Vlassova et
583 al. (2014) identified these same factors in their comparison of ASTER LST with MODIS LST
584 and Landsat LST with MODIS LST, respectively. Vlassova et al. (2014) found good
585 agreements between MODIS and Landsat LST, obtaining higher LST with MODIS LST to be
586 higher than with Landsat LST, which they attributed to the delay of 15 minutes in acquisition
587 time between MODIS and Landsat. MODIS LST is measured 15 minutes later and our results
588 showed that MODIS LSTs were indeed higher than Landsat LST. A comparison of MODIS
589 LST with locally measured canopy surface temperatures during the overpass time of MODIS
590 also showed agreement (Supporting information S7, Figure S7.1). The slope was possibly due

591 to differences in instrumentation and emissivity corrections and to scale issues, still this
592 comparison could corroborate the quality check of MODIS LST.

593 As the MODIS LST product is proven to be accurate within 1 °C (Silvério et al., 2015; Wan et
594 al., 2004) and has been intensively validated, the use of MODIS LST was a proper way to assess
595 the quality of our Landsat LST.

596

597 The errors from the different sources (such as atmospheric correction, emissivity correction,
598 resampling Landsat to MODIS resolution) are difficult to quantify. When we tested the impact
599 of atmospheric correction and emissivity errors on the LST from Landsat retrieval we found
600 that: (a) the overall patterns across different land use types did not change, (b) emissivity was
601 the most important factor, but the effects on LST retrieval were small and (c) errors due to
602 atmospheric correction parameters were small because there were ~~small~~ minor differences
603 between default Atmospheric correction (ATCOR) parameters and ATCOR parameters derived
604 with actual local conditions (relative humidity (RH), air pressure and air temperature).
605 Following the method of Coll et al. (2009) and Jiang et al. (2015) we show that the use of the
606 online atmospheric correction parameter calculator is a good option provided that RH, air
607 temperature and air pressure measurements are available. We additionally compared locally
608 measured air temperatures with MODIS air temperature and found a good agreement
609 (Supporting information S8, Figure S8.1), which served as a verification that we used a correct
610 air temperature for the atmospheric correction parameter calculator.

611 Overall, our comparison of LST from Landsat against LST from MODIS ~~as well as and~~ against
612 ground observations s suggests that we are able to retrieve meaningful spatial and temporal
613 patterns of LST in the Jambi province.

614

615 **4.2 LST patterns across different land use and land cover (LULC) types**

616

617 The land cover types in our study covered a range of land surface types that develop after forest
618 conversion. This is the first study in this region that includes oil palm and rubber as land use
619 types that develop after forest conversion. The coolest temperatures were at the vegetated land
620 cover types while the warmest surface temperatures were on the non-vegetated surface types
621 like urban areas and bare land. Interestingly, the oil palm and rubber plantations were only
622 slightly warmer than the forests whereas the young oil palm plantations had clearly higher LST
623 than the other vegetated surfaces. For other parts of the world, Lim et al. (2005, 2008), Fall et
624 al. (2010) and Weng et al. (2004) also observed cooler temperatures for forests and the highest
625 surface temperatures for barren and urban areas.

626 In Indonesia, land transformation is often not instantaneous from forest to oil palm or rubber
627 plantation, but can be associated with several years of bare or abandoned land in-between (Sheil
628 et al., 2009). Oil palm plantations typically have a rotation cycle of 25 years, resulting in
629 repeating patterns with young plantations (Dislich et al., 2016). Given the large differences in
630 LST between forests and bare soils or young oil palm plantations that we observed, a substantial
631 warming effect of land transformation at regional scale is expected.

632
633

634 **4.3 Drivers of local differences between different land cover types**

635

636 All land cover types (except Acacia Plantation Forests) had a higher albedo than forest,
637 indicating that these land cover types absorbed less incoming solar radiation than forests.
638 Nevertheless, these land cover types were warmer than forests, suggesting that the albedo was
639 not the dominant variable explaining LST. Indeed, the statistical analysis showed that $ET \sim$
640 LST had a higher correlation than $albedo \sim LST$. The ΔET s were significant, underlying that
641 despite their higher albedo, all land cover types had higher LSTs than forests due to lower ET
642 rates than forests. Vice versa, forests that absorb more solar radiation due to the lower albedo,

643 have lower LST due to the higher ET they exhibit, hereby identifying evaporative cooling as
644 the main determinant of regulating the surface temperature of all vegetation cover types (Li et
645 al., 2015).

646

647 Both observational and modeling studies carried out in other geographic regions and with other
648 trajectories support our observations. Observational studies in the Amazonia by Lawrence and
649 Vandecar (2015) on the conversion of natural vegetation to crop or pasture land showed a
650 surface warming effect. Salazar et al. (2015) provided additional evidence that conversion of
651 forest to other types of land use in the Amazonia caused significant reductions in precipitation
652 and increases in surface temperatures.

653 Alkama and Cescatti (2016) and earlier studies by Loarie et al. (2011a, 2011b) showed that
654 tropical deforestation may increase LST. Croplands in the Amazonian regions were also
655 warmer than forests through the reduction of ET (Ban-Weiss et al., 2011; Feddema et al., 2005)
656 and that the climatic response strongly depends on changes in energy fluxes rather than on
657 albedo changes (Loarie et al., 2011a, 2011b). A study by Silvério et al. (2015) indeed found
658 that tropical deforestation changes the surface energy balance and water cycle and that the
659 magnitude of the change strongly depends on the land uses that follow deforestation. They
660 found that the LST was 6.4 °C higher over croplands 6.4 °C higher and over pasture lands 4.3
661 °C higher over pasture lands compared to the forest they replaced, caused by a consequence
662 of energy balance shifts. Ban-Weiss et al. (2011) and Davin and de Noblet-Ducoudré (2010)
663 added that in addition to the reduction of ET, the reduction of surface roughness most likely
664 enhanced the substantial local warming.

665

666 Also for non-Amazonian regions, the replacement of forests by crops resulted in changes
667 comparable with similar to our observations. In temperate Argentina, Houspanossian et al.
668 (2013) found that the replacement of dry forests by crops resulted in an increase of albedo and

669 still ~~the~~ forests exhibited cooler canopies than croplands. The cooler canopies were a result of
670 ~~the a~~ higher aerodynamic conductance ~~that caused by that enhanced~~ the capacity of tree canopies
671 to dissipate heat into the atmosphere, and ~~to that~~ both latent and sensible heat fluxes operating
672 simultaneously ~~to~~ cooling forest canopies (~~Houspanossian et al. (2013)~~).

673

674 In a global analysis Li et al. (2015) showed that tropical forests generally have a low albedo,
675 but still the net energy gain caused by solar energy absorption is offset by a greater latent heat
676 loss via higher ET, and that in the tropical forests the high ET cooling completely offsets the
677 albedo warming. For China, this cooling effect was also shown by Peng et al. (2014) who
678 compared LST, albedo and ET of plantation forests, grassland and cropland with forests.

679

680 For the USA, Weng et al. (2004) and for China, Yue et al. (2007), ~~using~~ NDVI as an
681 ~~indicator of~~ vegetation abundance, ~~indicator and~~ also found ~~that~~ areas with a high mean NDVI
682 ~~to have had a~~ lower LST than areas with a low mean NDVI, ~~therefore, all~~ suggesting that
683 vegetation abundance is an important factor in controlling the LST through higher ET rates.
684 Our result support their assumptions by showing the high correlation between NDVI – LST and
685 ET – LST.

686

687 Our findings are also supported by modelling studies. Beltrán-Przekurat et al. (2012) found for
688 the Southern Amazon that conversion of wooded vegetation to soy bean plantations caused an
689 increase of the LST due to decreased latent heat and increased sensible heat fluxes. Climate
690 models also show the same warming trends and land surface modelling also projects an increase
691 in surface temperatures following deforestation in the Brazilian Cerrado (Beltrán-Przekurat et
692 al., 2012; Loarie et al., 2011b). In a global analysis, Pongratz et al. (2006) showed ~~a the~~ LST
693 increase of forest to cropland or pasture transitions, ~~also which was~~ driven by ~~a~~ reduced
694 roughness length ~~and, an~~ increased aerodynamic resistance, and that the temperature response

695 is intensified in forest to clear ~~land or~~/bare land transitions (1.2 – 1.7 °C increase). Similar to
696 observational studies, the modelling results of Bathiany et al. (2010) show that ET is the main
697 driver of temperature changes in tropical land areas.

698

699 In order to understanding the effects of deforestation on biophysical variables in Indonesia, our
700 study identifies the following mechanisms: (a) reduction of ET decreases surface cooling, (b)
701 reduced surface roughness reduces air mixing in the surface layer and thus vertical heat fluxes,
702 (c) changes in albedo change the net radiation, (d) changes in energy partitioning in sensible
703 and latent heat and heat storage. The effect is an increase of the mean temperatures leading to
704 warming effects in all tropical climatic zones (Alkama and Cescatti, 2016). We point here that
705 our study (1) included a ground heat flux, but did not take into account the storage of heat in
706 the soil and the release of stored heat out of the soil during the daily cycle and (2) that the
707 Landsat satellite image was obtained under cloud free conditions with high shortwave radiation
708 input and low fraction of diffuse radiation. Therefore, the LST retrieved on cloud free days
709 might be overestimated compared to cloudy days, where-as the differences in LST between land
710 uses are supposed to be loweress when diffuse radiation increases.

711

712 Our study is the first to include the oil palm and rubber expansion in Indonesia. In Indonesia,
713 smallholders take 40% of the land under oil palm cultivation for their account (Dislich et al.,
714 2016). Since the landscape in the Jambi province is characterized by small-scale smallholder-
715 dominated mosaic including rubber and oil palm monocultures (Clough et al., 2016), studies
716 using medium to coarse resolution data are not able to capture the small scale changes and
717 processes at the small-scale level. By using high resolution Landsat data we were able to also
718 include the effects of land use change on biophysical variables and the underlying processes of
719 the small scale holder agriculture.

720

721 4.4 Effects of land use change on the provincial surface temperature in the past decades

722

723 The increases in mean surface temperature of the Jambi province ~~increased~~were stronger
724 during the morning (10:30 am) and afternoon (1:30 pm) than during the evening (10:30 pm)
725 and night (1:30 am). Given that our results show a decrease of the NDVI in the same period,
726 this suggests that the observed increased trend of the day time province LST can be attributed
727 to the land cover changes that occurred. Our assumption that the observed decreasing NDVI
728 trend is caused by land conversions is supported by two different studies which reported that in
729 the Jambi province, between 2000 and 2011 (Drescher et al., 2016) and between 2000 and 2013
730 (Clough et al., 2016), the forest area decreased and that the largest increases were for rubber,
731 oil palm, and agricultural and tree crop areas. The class ‘other land use types’, which includes
732 urban areas, showed a minor increase (around 1%), ~~which suggests~~ings that the decrease in
733 NDVI was most likely caused by forest cover loss and not by urban expansion (see Supporting
734 information, Table S9). The same observations on LULC change in Indonesia were also
735 supported by Lee et al. (2011), Margono et al. (2012, 2014), ~~Paterson et al. (2015)~~ and Luskin
736 et al. (2014). Luskin et al. (2014) showed that in the Jambi province, during the period 2000
737 – 2010, forests decreased by 17% while, oil palm and rubber area increased by 85% and 19%,
738 respectively, in the Jambi province.

739

740 Given these trends in LULC changes, the observed LST trends were most likely caused by
741 gradual decrease of forest cover loss at the expense of agriculture and croplands. Our
742 assumptions are supported by findings of Silvério et al. (2015), Costa et al. (2007), Oliveira et
743 al. (2013), Spracklen et al. (2012) and Salazar et al. (2015) which indicate that land use
744 transitions in deforested areas likely have a strong influence on regional climate. Alkama and
745 Cescatti's (2016) analysis show that biophysical effects of changes in forest cover can
746 substantially affect the local climate by altering the average temperature, which is consistent

747 with our observations and can be related to the observed land use change in the Jambi province.
748 As Indonesia has undergone high rates of forest cover loss from 2000 to 2012 (Margono et al.,
749 2014), these findings support our assumptions that the observed LST increase in the Jambi
750 province was most likely caused by the observed land use changes.

751
752 To separate the effect of global warming from land-use change induced warming, we
753 considered areas with permanent and large enough forests as reference where changes are
754 mainly due to global warming. We find that LST of forests show either no significant trends (at
755 1:30 pm, 10:30 pm, 1:30 am) or just a clearly smaller increase of 0.03 °C per year at 10:30 am.
756 The difference between the LST trend of the province and of the forest at 10:30 am was 0.04
757 °C per year, resulting in a Δ LST of 0.6 °C between the province and forest in the period 2000
758 and 2015. We like to point out that our MODIS analysis has a larger proportion of data from
759 the dry season compared from the wet season, as there were more cloud free conditions during
760 the dry season. Thus, our reported warming effect reflects cloud free conditions. During cloudy
761 conditions, particularly in the wet season, the warming effect is expected to be lower. A
762 seasonality analysis showed that the relationships in the dry season are stronger than for the wet
763 season (see Supporting information S10, fig. S10.1) which suggests that the warming is more
764 pronounced during the dry season compared to the wet season, which is reasonable as we have
765 more incoming radiation during the dry season.

766
767 Using the warming effects we found between forest and other land cover types (Δ LST, Fig. 4a)
768 and the observed land cover changes by Clough et al. (2016), Drescher et al. (2016) (Supporting
769 Information S9, table S9.1 and S9.2) we estimated the contribution of all land cover types
770 (except forest) to the Δ LST of the province between 2000 and 2015 to be 0.51°C out of 0.6°C
771 observed above, which also supports our assumption that the increase of the province LST was
772 by 85% driven by land cover changes (see Supporting Information 9, Table S9.1 & S9.2: Land

773 use change analysis), with clear cut areas having a large contribution as they have the largest
774 warming effect.

775

776 The observed small, but significant increase in LST of forests ~~by of~~ 0.03 °C per year at 10:30
777 am reflects a LST change independent to land cover changes, as the forest remained unchanged
778 over that time period. ~~A p~~Potential driver of that LST increase is the general global air
779 temperature trend due to changes in radiative forcing or border effects (advection from warmer
780 land uses), which is similar to the 1994 - 2014 time series analysis of Kayet et al. (2016), –
781 who showed a LST increase for all land cover types ranging from wasted land, agriculture land,
782 open forest, dense forest, water bodies ~~and~~, built up ~~areas~~.

783

784 The observed trends of province air temperature (Fig. 5f) were significant, suggesting that a
785 general warming due to global and regional effects contributes to the observed warming at
786 province level during day and night time, but ~~that it~~ is smaller than the land cover change
787 induced effects (Supporting Information S9, Table S9.1 & S9.2) at provincial level (Fig. 5a and
788 5b).

789

790 In our ~~long term~~long-term analysis on the regional effects of land use change we observed an
791 increase in the mean LST and mean air temperature in the 2000 - 2015 period, concurrent ~~to~~
792 ~~with~~ a decrease of the NDVI. The warming observed from MODIS LST data and from the air
793 temperature obtained from the independent ERA Interim Reanalysis in the Jambi province are
794 most likely caused by the observed decrease of the forest area and an increase oil palm, rubber
795 and other cash crop areas in the same period, with other effects such as radiative forcing changes
796 and additional natural effects playing a smaller role. Given the plan of the Indonesian
797 government~~al~~ to substantially expand oil palm ~~productivity~~production with an projected
798 additional demand of 1 to 28 Mha in 2020 (Wicke et al., 2011), the strong warming effect we

799 show for Jambi province may serve as an indication of future changes in LST for other regions
800 of Indonesia that will undergo land transformations towards oil palm plantations.

801 A recent study by Tölle et al. (2017) showed that for Southeast Asia, as a whole that land use
802 change at large scale may increase not only surface temperature but also impact other aspects
803 of local and regional weather and climate occurring also in regionsmes remote from the original
804 landscape disturbance. Their results also indicate that Land clearings can amplify the response
805 to climatic extreme events such as El Niño Southern Oscillation (ENSO). The observed effects
806 of land use change on the biophysical variables may have implications for ecosystem services
807 in the Jambi province beyond a pure warming effect. The high precipitation in this region in
808 combination with the reduced vegetation cover of bare land and young oil palm plantations
809 impose risks of soil erosion caused by surface run off. Less water infiltrates in the soil, thereby
810 decreasing the soil water storage that may lead to low water availability in the dry season
811 (Dislich et al., 2016; Merten et al., 2016). High surface temperatures in combination with low
812 water availability may make the vegetation and the surroundings more vulnerable ~~for~~to fires.

813

814 **5 Conclusion**

815

816 In summary, we showed the importance of forests in regulating the local and regional climate.
817 We derived biophysical variables from satellite data, analyzed the biophysical impacts of
818 deforestation and on a local scale we found a general warming effect after forests are
819 transformed to cash or tree croplands (oil palm, rubber, acacia) in the Jambi province of
820 Sumatra. The warming effect after forest conversion results from the reduced evaporative
821 cooling, which was identified as the main determinant of regulating the surface temperature.
822 On a regional scale, we saw that the effects of land cover changes are reflected back in changes
823 of the LST, NDVI and air temperature of the Jambi province. The warming effect induced by
824 land cover change clearly exceeded the global warming effect. Understanding the effects of

825 land cover change on the biophysical variables may support policies regarding conservation of
826 the existing forests, planning and expansion of the oil palm plantations and possible
827 afforestation measures.

828

829

830 **Supporting Information**

831

832 Supporting information to this article is arranged as follows:

833

834 **S1. Surface temperature retrieval from Landsat thermal images**

835 **Table S1.1.** Steps in the retrieval of the surface temperature from Landsat TIR band

836 **Table S1.2.** LMIN and LMAX values for Landsat 7 ETM+

837 **Table S1.3.** Mean solar exo-atmospheric irradiance ($ESUN_{\lambda}$) for Landsat 7 ETM+

838

839 **S2. Atmospheric correction of the thermal band**

840 **Table S2.1.** Input and output parameters for/from NASA's online atmospheric correction
841 parameter calculator

842

843 **S3. ET from satellite images with SEBAL**

844 **Fig. S3.1** Analysis of the steps involved in deriving the input for deriving ET from Landsat
845 images with SEBAL

846 **Fig. S3.2** Comparison of ET derived from upper anchor and lower anchor pixels.

847 **Table S3.1.** u^* , rah , LE and H measured at a young and mature oil palm plantation

848

849 **S4. Mean LST, NDVI, Albedo and NDVI extracted for 7 land cover types**

850 **Fig. S4.1** Mean LST, NDVI, Albedo and NDVI extracted from Landsat LST images for 7
851 land cover types

852

853 **S5. Difference in LST, NDVI, albedo and ET between Forest (FO) and 6 other land cover
854 types**

855 **Fig. S5.1** Differences in LST (ΔLST), NDVI ($\Delta NDVI$), Albedo ($\Delta Albedo$) and
856 Evapotranspiration (ΔET) between other land covers (RU, MOP, PF, YOP, UB and CLC) and
857 forest (FO) in the Jambi province

858

859 **S6. Statistical analysis**

860 **Table S6.1** ANOVA statistics

861 **Table S6.2** Post-hoc Tukey HSD test statistics

862 **Table S6.3** The relation LST-Albedo-NDVI-ET separated by land cover type

863

864 **S7. Comparison of MODIS LST to in situ measured canopy LST**

865 **Fig. S7.1** MODIS LST compared to in situ measured canopy surface temperature.

866

867 **S8. Comparison of MODIS Air temperature with locally measured air temperature**

868 **Fig. S8.1** MODIS Air temperature compared with in situ measured air temperatures

869

870 **S9. Land use change analysis for the Jambi province for 2000 – 2010**

871 **Table S9.1** Land use change (1990) – 2000 – 2010

872 **Table S9.2** Contribution of land cover change to total LST increase

873

874 **S10. Seasonality analysis**

875 **Fig. S10.1** Mean annual LST in the Jambi province between 2000 and 2015 derived from
876 MODIS LST during the wet and dry season.

877

878 *Author contributions.* Clifton R. Sabajo conducted the research, fieldwork an analysis and
879 prepared the manuscript, which was reviewed by Guerric le Maire, Tania June, Ana Meijide,
880 Olivier Roupsard and Alexander Knohl. Ana Meijide and Alexander Knohl provided the
881 meteorological data.

Competing interests. The authors declare that they have no conflict of interest.

882 *Acknowledgements.* This research was funded by the Erasmus Mundus Joint Doctorate
883 Programme Forest and Nature for Society (EMJD FONASO) and the German Research
884 Foundation (DFG) through the CRC 990 “EForTS, Ecological and Socioeconomic Functions
885 of Tropical Lowland Rainforest Transformation Systems (Sumatra, Indonesia)” (subproject
886 A03). A special thanks to Huta Julu Bagus Putra, a.k.a. Monang, for his assistance and
887 translation during the field work in Indonesia. The authors state to have no conflict of interest.

888

889

890 **References**

891

892 [Alkama, R. and Cescatti, A.: Biophysical climate impacts of recent changes in global forest](#)
893 [cover, Science, 351\(6273\), 600–604, doi:10.1126/science.aac8083, 2016.](#)

894 [Ban-Weiss, G. A., Bala, G., Cao, L., Pongratz, J. and Caldeira, K.: Climate forcing and response](#)
895 [to idealized changes in surface latent and sensible heat, Environ. Res. Lett., 6\(3\), 34032, 2011.](#)

896 [Barsi, J. A., Barker, J. L. and Schott, J. R.: An Atmospheric Correction Parameter Calculator](#)
897 [for a Single Thermal Band Earth-Sensing Instrument, Geosci. Remote Sens. Symp. 2003](#)
898 [IGARSS 03 Proc. 2003 IEEE Int., 5, 3014–3016 vol.5, doi:10.1109/IGARSS.2003.1294665,](#)
899 [2003.](#)

900 [Barsi, J. A., Schott, J. R., Palluconi, F. D. and Hook, S. J.: Validation of a web-based](#)
901 [atmospheric correction tool for single thermal band instruments, in Proc. SPIE, Earth Observing](#)
902 [Systems X, vol. 5882, San Diego, California, USA., 2005.](#)

903 [Bastiaanssen, W. G. .: SEBAL-based sensible and latent heat fluxes in the irrigated Gediz](#)
904 [Basin, Turkey, J. Hydrol., 229\(1–2\), 87–100, doi:10.1016/S0022-1694\(99\)00202-4, 2000.](#)

905 [Bastiaanssen, W. G. M., Menenti, M., Feddes, R. A. and Holtslag, A. A. M.: A remote sensing](#)
906 [surface energy balance algorithm for land \(SEBAL\) - 1. Formulation, J. Hydrol., 212\(1–4\),](#)
907 [198–212, doi:10.1016/s0022-1694\(98\)00253-4, 1998a.](#)

908 [Bastiaanssen, W. G. M., Pelgrum, H., Wang, J., Ma, Y., Moreno, J. F., Roerink, G. J. and van](#)
909 [der Wal, T.: A remote sensing surface energy balance algorithm for land \(SEBAL\): Part 2:](#)
910 [Validation, J. Hydrol., 212–213, 213–229, doi:10.1016/S0022-1694\(98\)00254-6, 1998b.](#)

911 [Bathiany, S., Claussen, M., Brovkin, V., Raddatz, T. and Gayler, V.: Combined biogeophysical](#)
912 [and biogeochemical effects of large-scale forest cover changes in the MPI earth system model,](#)
913 [Biogeosciences, 7\(5\), 1383–1399, doi:10.5194/bg-7-1383-2010, 2010.](#)

914 [Beltrán-Przekurat, A., Pielke Sr, R. A., Eastman, J. L. and Coughenour, M. B.: Modelling the](#)
915 [effects of land-use/land-cover changes on the near-surface atmosphere in southern South](#)
916 [America, Int. J. Climatol., 32\(8\), 1206–1225, doi:10.1002/joc.2346, 2012.](#)

917 [Bindhu, V. M., Narasimhan, B. and Sudheer, K. P.: Development and verification of a non-](#)
918 [linear disaggregation method \(NL-DisTrad\) to downscale MODIS land surface temperature to](#)
919 [the spatial scale of Landsat thermal data to estimate evapotranspiration, Remote Sens. Environ.,](#)
920 [135, 118–129, doi:10.1016/j.rse.2013.03.023, 2013.](#)

921 [Boisier, J. P., de Noblet-Ducoudré, N. and Ciais, P.: Historical land-use-induced](#)
922 [evapotranspiration changes estimated from present-day observations and reconstructed land-](#)
923 [cover maps, Hydrol. Earth Syst. Sci., 18\(9\), 3571–3590, doi:10.5194/hess-18-3571-2014, 2014.](#)

924 [Bridhikitti, A. and Overcamp, T. J.: Estimation of Southeast Asian rice paddy areas with](#)
925 [different ecosystems from moderate-resolution satellite imagery, Agric. Ecosyst. Environ.,](#)
926 [146\(1\), 113–120, doi:10.1016/j.agee.2011.10.016, 2012.](#)

927 [Bright, R. M., Zhao, K., Jackson, R. B. and Cherubini, F.: Quantifying surface albedo and other](#)
928 [direct biogeophysical climate forcings of forestry activities, Glob. Change Biol., 21\(9\), 3246–](#)
929 [3266, doi:10.1111/gcb.12951, 2015.](#)

930 [Clough, Y., Krishna, V. V., Corre, M. D., Darras, K., Denmead, L. H., Meijide, A., Moser, S.,](#)
931 [Musshoff, O., Steinebach, S., Veldkamp, E., Allen, K., Barnes, A. D., Breidenbach, N., Brose,](#)
932 [U., Buchori, D., Daniel, R., Finkeldey, R., Harahap, I., Hertel, D., Holtkamp, A. M., Hörandl,](#)
933 [E., Irawan, B., Jaya, I. N. S., Jochum, M., Klarner, B., Knohl, A., Kotowska, M. M.,](#)
934 [Krashevskaya, V., Kreft, H., Kurniawan, S., Leuschner, C., Maraun, M., Melati, D. N.,](#)
935 [Opfermann, N., Pérez-Cruzado, C., Prabowo, W. E., Rembold, K., Rizali, A., Rubiana, R.,](#)
936 [Schneider, D., Tjitrosoedirdjo, S. S., Tjoa, A., Tschardtke, T. and Scheu, S.: Land-use choices](#)
937 [follow profitability at the expense of ecological functions in Indonesian smallholder landscapes,](#)
938 [Nat. Commun., 7, 13137, 2016.](#)

939 [Coll, C., Wan, Z. and Galve, J. M.: Temperature-based and radiance-based validations of the](#)
940 [V5 MODIS land surface temperature product, J. Geophys. Res., 114\(D20\), 2009.](#)

941 [Coll, C., Galve, J. M., Sanchez, J. M. and Caselles, V.: Validation of Landsat-7/ETM+ Thermal-](#)
942 [Band Calibration and Atmospheric Correction With Ground-Based Measurements, Geosci.](#)
943 [Remote Sens. IEEE Trans. On, 48\(1\), 547–555, doi:10.1109/TGRS.2009.2024934, 2010.](#)

944 [Costa, M. H., Yanagi, S. N. M., Souza, P. J. O. P., Ribeiro, A. and Rocha, E. J. P.: Climate](#)
945 [change in Amazonia caused by soybean cropland expansion, as compared to caused by](#)
946 [pastureland expansion, Geophys. Res. Lett., 34\(7\), doi:10.1029/2007GL029271, 2007.](#)

947 [Davin, E. L. and de Noblet-Ducoudré, N.: Climatic Impact of Global-Scale Deforestation:](#)
948 [Radiative versus Nonradiative Processes, J. Clim., 23\(1\), 97–112,](#)
949 [doi:10.1175/2009JCLI3102.1, 2010.](#)

950 [Dee, D. P., Uppala, S. M., Simmons, A. J., Berrisford, P., Poli, P., Kobayashi, S., Andrae, U.,](#)
951 [Balmaseda, M. A., Balsamo, G., Bauer, P., Bechtold, P., Beljaars, A. C. M., van de Berg, L.,](#)
952 [Bidlot, J., Bormann, N., Delsol, C., Dragani, R., Fuentes, M., Geer, A. J., Haimberger, L.,](#)
953 [Healy, S. B., Hersbach, H., Hólm, E. V., Isaksen, L., Kållberg, P., Köhler, M., Matricardi, M.,](#)
954 [McNally, A. P., Monge-Sanz, B. M., Morcrette, J.-J., Park, B.-K., Peubey, C., de Rosnay, P.,](#)
955 [Tavolato, C., Thépaut, J.-N. and Vitart, F.: The ERA-Interim reanalysis: configuration and](#)
956 [performance of the data assimilation system, Q. J. R. Meteorol. Soc., 137\(656\), 553–597,](#)
957 [doi:10.1002/qj.828, 2011.](#)

958 [Dislich, C., Keyel, A. C., Salecker, J., Kisel, Y., Meyer, K. M., Auliya, M., Barnes, A. D.,](#)
959 [Corre, M. D., Darras, K., Faust, H., Hess, B., Klasen, S., Knohl, A., Kreft, H., Meijide, A.,](#)
960 [Nurdiansyah, F., Otten, F., Pe’er, G., Steinebach, S., Tarigan, S., Tölle, M. H., Tschardtke, T.](#)
961 [and Wiegand, K.: A review of the ecosystem functions in oil palm plantations, using forests as](#)
962 [a reference system, Biol. Rev., doi:10.1111/brv.12295, 2016.](#)

963 [Drescher, J., Rembold, K., Allen, K., Beckschäfer, P., Buchori, D., Clough, Y., Faust, H., Fauzi,](#)
964 [A. M., Gunawan, D., Hertel, D., Irawan, B., Jaya, I. N. S., Klarner, B., Kleinn, C., Knohl, A.,](#)
965 [Kotowska, M. M., Krashevskaya, V., Krishna, V., Leuschner, C., Lorenz, W., Meijide, A., Melati,](#)
966 [D., Nomura, M., Pérez-Cruzado, C., Qaim, M., Siregar, I. Z., Steinebach, S., Tjoa, A.,](#)
967 [Tschardtke, T., Wick, B., Wiegand, K., Kreft, H. and Scheu, S.: Ecological and socio-economic](#)
968 [functions across tropical land use systems after rainforest conversion, Philos. Trans. R. Soc.](#)
969 [Lond. B Biol. Sci., 371\(1694\), doi:10.1098/rstb.2015.0275, 2016.](#)

970 [Fall, S., Niyogi, D., Gluhovsky, A., Pielke, R. A., Kalnay, E. and Rochon, G.: Impacts of land](#)
971 [use land cover on temperature trends over the continental United States: assessment using the](#)
972 [North American Regional Reanalysis, Int. J. Climatol., 30\(13\), 1980–1993,](#)
973 [doi:10.1002/joc.1996, 2010.](#)

974 [Feddema, J. J., Oleson, K. W., Bonan, G. B., Mearns, L. O., Buja, L. E., Meehl, G. A. and](#)
975 [Washington, W. M.: The Importance of Land-Cover Change in Simulating Future Climates,](#)
976 [Science, 310\(5754\), 1674, doi:10.1126/science.1118160, 2005.](#)

977 [Hoffmann, W. A. and Jackson, R. B.: Vegetation–Climate Feedbacks in the Conversion of](#)
978 [Tropical Savanna to Grassland, J. Clim., 13\(9\), 1593–1602, doi:10.1175/1520-](#)
979 [0442\(2000\)013<1593:VCFITC>2.0.CO;2, 2000.](#)

980 [Houspanossian, J., Nosetto, M. and Jobbágy, E. G.: Radiation budget changes with dry forest](#)
981 [clearing in temperate Argentina, Glob. Change Biol., 19\(4\), 1211–1222,](#)
982 [doi:10.1111/gcb.12121, 2013.](#)

983 [Idso, S. B. and Jackson, R. D.: Thermal radiation from the atmosphere, J. Geophys. Res.,](#)
984 [74\(23\), 5397–5403, doi:10.1029/JC074i023p05397, 1969.](#)

985 [Jiang, Y., Fu, P. and Weng, Q.: Assessing the Impacts of Urbanization-Associated Land](#)
986 [Use/Cover Change on Land Surface Temperature and Surface Moisture: A Case Study in the](#)
987 [Midwestern United States, Remote Sens., 7\(4\), doi:10.3390/rs70404880, 2015.](#)

988 [Kayet, N., Pathak, K., Chakrabarty, A. and Sahoo, S.: Spatial impact of land use/land cover](#)
989 [change on surface temperature distribution in Saranda Forest, Jharkhand, Model. Earth Syst.](#)
990 [Environ., 2\(3\), 1–10, doi:10.1007/s40808-016-0159-x, 2016.](#)

991 [Lawrence, D. and Vandecar, K.: Effects of tropical deforestation on climate and agriculture,](#)
992 [Nat. Clim. Change, 5\(1\), 27–36, 2015.](#)

993 [Lee, X., Goulden, M. L., Hollinger, D. Y., Barr, A., Black, T. A., Bohrer, G., Bracho, R., Drake,](#)
994 [B., Goldstein, A., Gu, L., Katul, G., Kolb, T., Law, B. E., Margolis, H., Meyers, T., Monson,](#)
995 [R., Munger, W., Oren, R., Paw U, K. T., Richardson, A. D., Schmid, H. P., Staebler, R., Wofsy,](#)
996 [S. and Zhao, L.: Observed increase in local cooling effect of deforestation at higher latitudes,](#)
997 [Nature, 479\(7373\), 384–387, doi:10.1038/nature10588, 2011.](#)

998 [van Leeuwen, T. T., Frank, A. J., Jin, Y., Smyth, P., Goulden, M. L., van der Werf, G. R. and](#)
999 [Randerson, J. T.: Optimal use of land surface temperature data to detect changes in tropical](#)
1000 [forest cover, J. Geophys. Res. Biogeosciences, 116\(G2\), doi:10.1029/2010JG001488, 2011.](#)

1001 [Li, F., Jackson, T. J., Kustas, W. P., Schmugge, T. J., French, A. N., Cosh, M. H. and Bindlish,](#)
1002 [R.: Deriving land surface temperature from Landsat 5 and 7 during SMEX02/SMACEX, 2002](#)
1003 [Soil Moisture Exp. SMEX02, 92\(4\), 521–534, doi:10.1016/j.rse.2004.02.018, 2004.](#)

1004 [Li, Y., Zhao, M., Motesharrei, S., Mu, Q., Kalnay, E. and Li, S.: Local cooling and warming](#)
1005 [effects of forests based on satellite observations, Nat. Commun., 6 \[online\] Available from:](#)
1006 [http://dx.doi.org/10.1038/ncomms7603, 2015.](#)

1007 [Liang, S.: Narrowband to broadband conversions of land surface albedo I: Algorithms, Remote](#)
1008 [Sens. Environ., 76\(2\), 213–238, doi:10.1016/S0034-4257\(00\)00205-4, 2000.](#)

1009 [Lim, Y.-K., Cai, M., Kalnay, E. and Zhou, L.: Observational evidence of sensitivity of surface](#)
1010 [climate changes to land types and urbanization, Geophys. Res. Lett., 32\(22\),](#)
1011 [doi:10.1029/2005GL024267, 2005.](#)

1012 [Lim, Y.-K., Cai, M., Kalnay, E. and Zhou, L.: Impact of Vegetation Types on Surface](#)
1013 [Temperature Change, J. Appl. Meteorol. Climatol., 47\(2\), 411–424, 2008.](#)

- 1014 [Loarie, S. R., Lobell, D. B., Asner, G. P., Mu, Q. and Field, C. B.: Direct impacts on local](#)
1015 [climate of sugar-cane expansion in Brazil, Nat. Clim. Change, 1\(2\), 105–109,](#)
1016 [doi:10.1038/nclimate1067, 2011a.](#)
- 1017 [Loarie, S. R., Lobell, D. B., Asner, G. P. and Field, C. B.: Land-Cover and Surface Water](#)
1018 [Change Drive Large Albedo Increases in South America, Earth Interact., 15\(7\), 1–16, 2011b.](#)
- 1019 [Longobardi, P., Montenegro, A., Beltrami, H. and Eby, M.: Deforestation Induced Climate](#)
1020 [Change: Effects of Spatial Scale, PLoS ONE, 11\(4\), e0153357,](#)
1021 [doi:10.1371/journal.pone.0153357, 2016.](#)
- 1022 [Luskin, M. S., Christina, E. D., Kelley, L. C. and Potts, M. D.: Modern Hunting Practices and](#)
1023 [Wild Meat Trade in the Oil Palm Plantation-Dominated Landscapes of Sumatra, Indonesia,](#)
1024 [Hum. Ecol., 42\(1\), 35–45, doi:10.1007/s10745-013-9606-8, 2014.](#)
- 1025 [Mahmood, R., Pielke, R. A., Hubbard, K. G., Niyogi, D., Dirmeyer, P. A., McAlpine, C.,](#)
1026 [Carleton, A. M., Hale, R., Gameda, S., Beltrán-Przekurat, A., Baker, B., McNider, R., Legates,](#)
1027 [D. R., Shepherd, M., Du, J., Blanken, P. D., Frauenfeld, O. W., Nair, U. S. and Fall, S.: Land](#)
1028 [cover changes and their biogeophysical effects on climate, Int. J. Climatol., 34\(4\), 929–953,](#)
1029 [doi:10.1002/joc.3736, 2014.](#)
- 1030 [Margono, B. A., Turubanova, S., Zhuravleva, I., Potapov, P., Tyukavina, A., Baccini, A., Goetz,](#)
1031 [S. and Hansen, M. C.: Mapping and monitoring deforestation and forest degradation in Sumatra](#)
1032 [\(Indonesia\) using Landsat time series data sets from 1990 to 2010, Environ. Res. Lett., 7\(3\),](#)
1033 [34010, doi:10.1088/1748-9326/7/3/034010, 2012.](#)
- 1034 [Margono, B. A., Potapov, P. V., Turubanova, S., Stolle, F. and Hansen, M. C.: Primary forest](#)
1035 [cover loss in Indonesia over 2000-2012, Nat. Clim Change, 4\(8\), 730–735, 2014.](#)
- 1036 [Marlier, M. E., DeFries, R., Pennington, D., Nelson, E., Ordway, E. M., Lewis, J., Koplitz, S.](#)
1037 [N. and Mickley, L. J.: Future fire emissions associated with projected land use change in](#)
1038 [Sumatra, Glob. Change Biol., 21\(1\), 345–362, doi:10.1111/gcb.12691, 2015.](#)
- 1039 [Meijide, A., Röhl, A., Fan, Y., Herbst, M., Niu, F., Tiedemann, F., June, T., Rauf, A., Hölscher,](#)
1040 [D. and Knohl, A.: Controls of water and energy fluxes in oil palm plantations: Environmental](#)
1041 [variables and oil palm age, Agric. For. Meteorol., 239, 71–85,](#)
1042 [doi:10.1016/j.agrformet.2017.02.034, 2017.](#)
- 1043 [Merten, J., Röhl, A., Guillaume, T., Meijide, A., Tarigan, S., Agusta, H., Dislich, C., Dittrich,](#)
1044 [C., Faust, H., Gunawan, D., Hein, J., Hendrayanto, Knohl, A., Kuzyakov, Y., Wiegand, K. and](#)
1045 [Hölscher, D.: Water scarcity and oil palm expansion: social views and environmental processes,](#)
1046 [Ecol. Soc., 21\(2\), doi:10.5751/ES-08214-210205, 2016.](#)
- 1047 [Miettinen, J., Shi, C. and Liew, S. C.: Deforestation rates in insular Southeast Asia between](#)
1048 [2000 and 2010, Glob. Change Biol., 17\(7\), 2261–2270, 2011.](#)
- 1049 [Miettinen, J., Hooijer, A., Wang, J., Shi, C. and Liew, S. C.: Peatland degradation and](#)
1050 [conversion sequences and interrelations in Sumatra, Reg. Environ. Change, 12\(4\), 729–737,](#)
1051 [doi:10.1007/s10113-012-0290-9, 2012.](#)

- 1052 [Mildrexler, D. J., Zhao, M. and Running, S. W.: A global comparison between station air](#)
1053 [temperatures and MODIS land surface temperatures reveals the cooling role of forests, J.](#)
1054 [Geophys. Res. Biogeosciences, 116\(G3\), doi:10.1029/2010JG001486, 2011.](#)
- 1055 [Nosetto, M. D., Jobbágy, E. G. and Paruelo, J. M.: Land-use change and water losses: the case](#)
1056 [of grassland afforestation across a soil textural gradient in central Argentina, Glob. Change](#)
1057 [Biol., 11\(7\), 1101–1117, doi:10.1111/j.1365-2486.2005.00975.x, 2005.](#)
- 1058 [Oliveira, L. J. C., Costa, M. H., Soares-Filho, B. S. and Coe, M. T.: Large-scale expansion of](#)
1059 [agriculture in Amazonia may be a no-win scenario, Environ. Res. Lett., 8\(2\), 24021, 2013.](#)
- 1060 [Paterson, R. R. M., Kumar, L., Taylor, S. and Lima, N.: Future climate effects on suitability for](#)
1061 [growth of oil palms in Malaysia and Indonesia, Sci. Rep., 5, 14457, 2015.](#)
- 1062 [Peng, S.-S., Piao, S., Zeng, Z., Ciais, P., Zhou, L., Li, L. Z. X., Myneni, R. B., Yin, Y. and](#)
1063 [Zeng, H.: Afforestation in China cools local land surface temperature, Proc. Natl. Acad. Sci.,](#)
1064 [111\(8\), 2915–2919, 2014.](#)
- 1065 [Pongratz, J., Bounoua, L., DeFries, R. S., Morton, D. C., Anderson, L. O., Mauser, W. and](#)
1066 [Klink, C. A.: The Impact of Land Cover Change on Surface Energy and Water Balance in Mato](#)
1067 [Grosso, Brazil, Earth Interact., 10\(19\), 1–17, 2006.](#)
- 1068 [Salazar, A., Baldi, G., Hirota, M., Syktus, J. and McAlpine, C.: Land use and land cover change](#)
1069 [impacts on the regional climate of non-Amazonian South America: A review, Glob. Planet.](#)
1070 [Change, 128, 103–119, doi:10.1016/j.gloplacha.2015.02.009, 2015.](#)
- 1071 [Salazar, A., Katzfey, J., Thatcher, M., Syktus, J., Wong, K. and McAlpine, C.: Deforestation](#)
1072 [changes land–atmosphere interactions across South American biomes, Glob. Planet. Change,](#)
1073 [139, 97–108, doi:10.1016/j.gloplacha.2016.01.004, 2016.](#)
- 1074 [Sheil, D., Casson, A., Meijaard, E., Van Noordwijk, M., Gaskell, J., Sunderland-Groves, J.,](#)
1075 [Wertz, K. and Kanninen, M.: The impacts and opportunities of oil palm in Southeast Asia: What](#)
1076 [do we know and what do we need to know?, Center for International Forestry Research](#)
1077 [\(CIFOR\), Bogor, Indonesia., 2009.](#)
- 1078 [Silvério, D. V., Brando, P. M., Macedo, M. N., Beck, P. S. A., Bustamante, M. and Coe, M. T.:](#)
1079 [Agricultural expansion dominates climate changes in southeastern Amazonia: the overlooked](#)
1080 [non-GHG forcing, Environ. Res. Lett., 10\(10\), 104015, 2015.](#)
- 1081 [Snyder, W. C., Wan, Z., Zhang, Y. and Feng, Y.-Z.: Classification-based emissivity for land](#)
1082 [surface temperature measurement from space, Int. J. Remote Sens., 19\(14\), 2753–2774,](#)
1083 [doi:10.1080/014311698214497, 1998.](#)
- 1084 [Sobrino, J. A., Jiménez-Muñoz, J. C. and Paolini, L.: Land surface temperature retrieval from](#)
1085 [LANDSAT TM 5, Remote Sens. Environ., 90\(4\), 434–440, doi:10.1016/j.rse.2004.02.003,](#)
1086 [2004.](#)
- 1087 [Sobrino, J. A., Jiménez-Muñoz, J. C., Zarco-Tejada, P. J., Sepulcre-Cantó, G. and de Miguel,](#)
1088 [E.: Land surface temperature derived from airborne hyperspectral scanner thermal infrared data,](#)
1089 [Remote Sens. Environ., 102\(1–2\), 99–115, doi:10.1016/j.rse.2006.02.001, 2006.](#)
- 1090 [Sobrino, J. A., Jimenez-Muoz, J. C., Soria, G., Romaguera, M., Guanter, L., Moreno, J., Plaza,](#)
1091 [A. and Martinez, P.: Land Surface Emissivity Retrieval From Different VNIR and TIR Sensors,](#)

1092 [Geosci. Remote Sens. IEEE Trans. On, 46\(2\), 316–327, doi:10.1109/TGRS.2007.904834,](#)
1093 [2008.](#)

1094 [Spracklen, D. V., Arnold, S. R. and Taylor, C. M.: Observations of increased tropical rainfall](#)
1095 [preceded by air passage over forests, Nature, 489\(7415\), 282–285, doi:10.1038/nature11390,](#)
1096 [2012.](#)

1097 [Tölle, M. H., Engler, S. and Panitz, H.-J.: Impact of Abrupt Land Cover Changes by Tropical](#)
1098 [Deforestation on Southeast Asian Climate and Agriculture, J. Clim., 30\(7\), 2587–2600,](#)
1099 [doi:10.1175/JCLI-D-16-0131.1, 2017.](#)

1100 [Verstraeten, W. W., Veroustraete, F. and Feyen, J.: Estimating evapotranspiration of European](#)
1101 [forests from NOAA-imagery at satellite overpass time: Towards an operational processing](#)
1102 [chain for integrated optical and thermal sensor data products, Remote Sens. Environ., 96\(2\),](#)
1103 [256–276, doi:10.1016/j.rse.2005.03.004, 2005.](#)

1104 [Vlassova, L., Perez-Cabello, F., Nieto, H., Martín, P., Riaño, D. and de la Riva, J.: Assessment](#)
1105 [of Methods for Land Surface Temperature Retrieval from Landsat-5 TM Images Applicable to](#)
1106 [Multiscale Tree-Grass Ecosystem Modeling, Remote Sens., 6\(5\), doi:10.3390/rs6054345,](#)
1107 [2014.](#)

1108 [Voogt, J. A. and Oke, T. R.: Effects of urban surface geometry on remotely-sensed surface](#)
1109 [temperature, Int. J. Remote Sens., 19\(5\), 895–920, doi:10.1080/014311698215784, 1998.](#)

1110 [Wan, Z., Zhang, Y., Zhang, Q. and Li, Z.-L.: Quality assessment and validation of the MODIS](#)
1111 [global land surface temperature, Int. J. Remote Sens., 25\(1\), 261–274,](#)
1112 [doi:10.1080/0143116031000116417, 2004.](#)

1113 [Weng, Q.: Thermal infrared remote sensing for urban climate and environmental studies:](#)
1114 [Methods, applications, and trends, ISPRS J. Photogramm. Remote Sens., 64\(4\), 335–344,](#)
1115 [doi:10.1016/j.isprsjprs.2009.03.007, 2009.](#)

1116 [Weng, Q., Lu, D. and Schubring, J.: Estimation of land surface temperature–vegetation](#)
1117 [abundance relationship for urban heat island studies, Remote Sens. Environ., 89\(4\), 467–483,](#)
1118 [doi:10.1016/j.rse.2003.11.005, 2004.](#)

1119 [Wicke, B., Sikkema, R., Dornburg, V. and Faaij, A.: Exploring land use changes and the role](#)
1120 [of palm oil production in Indonesia and Malaysia, Land Use Policy, 28\(1\), 193–206, 2011.](#)

1121 [Wukelic, G. E., Gibbons, D. E., Martucci, L. M. and Foote, H. P.: Radiometric calibration of](#)
1122 [Landsat Thematic Mapper thermal band, Remote Sens. Environ., 28\(0\), 339–347,](#)
1123 [doi:10.1016/0034-4257\(89\)90125-9, 1989.](#)

1124 [Yue, W., Xu, J., Tan, W. and Xu, L.: The relationship between land surface temperature and](#)
1125 [NDVI with remote sensing: application to Shanghai Landsat 7 ETM+ data, Int. J. Remote Sens.,](#)
1126 [28\(15\), 3205–3226, doi:10.1080/01431160500306906, 2007.](#)

1127 [Zhang, Z. and He, G.: Generation of Landsat surface temperature product for China, 2000–](#)
1128 [2010, Int. J. Remote Sens., 34\(20\), 7369–7375, doi:10.1080/01431161.2013.820368, 2013.](#)

1129 [Zhou, X. and Wang, Y.-C.: Dynamics of Land Surface Temperature in Response to Land-](#)
1130 [Use/Cover Change, Geogr. Res., 49\(1\), 23–36, doi:10.1111/j.1745-5871.2010.00686.x, 2011.](#)

1131

1132

